

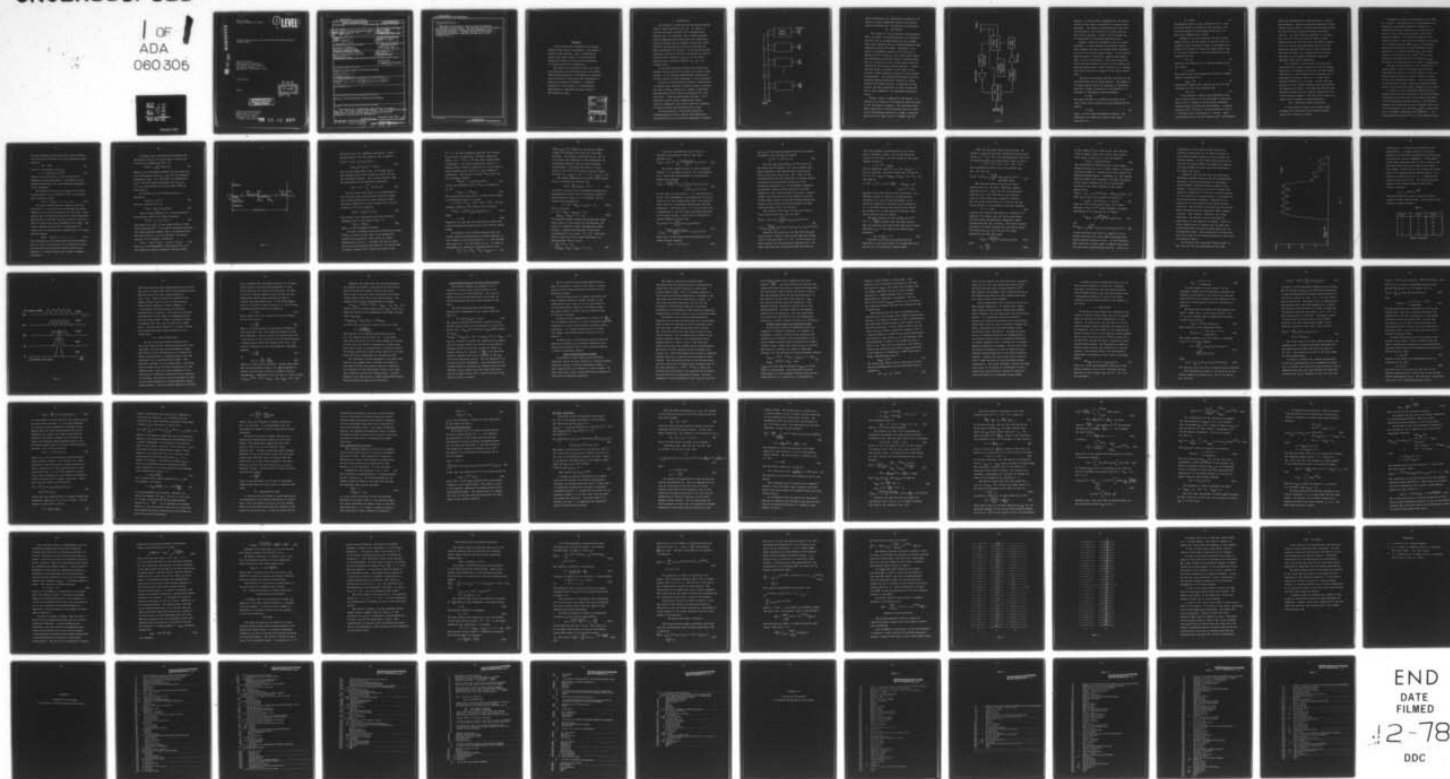
AD-A060 305

MINNESOTA UNIV MINNEAPOLIS DEPT OF ELECTRICAL ENGIN--ETC F/G 17/1
A NOVEL CONCEPT FOR A SELF-FOCUSING AND TARGET SEEKING SONAR SY--ETC(U)
MAY 78 R K MUELLER N00014-75-C-0631

UNCLASSIFIED

NL

1 OF 1
ADA
060 305



END
DATE
FILMED
2-78
DDC

AD A060305

DDC FILE COPY

Final Report
Contract N00014-75-C-0631

5130178 BK
①

LEVEL III

A NOVEL CONCEPT FOR A SELF-FOCUSING AND TARGET SEEKING
SONAR SYSTEM

Rolf K. Mueller
University of Minnesota
139 Electrical Engineering
123 Church Street, S.E.
Minneapolis, Minnesota 55455

16 May 1978

Final

DDC
RECEIVED
OCT 24 1978
B

DISTRIBUTION STATEMENT A

Approved for public release;
Distribution Unlimited

Office of Naval Research
Department of the Navy
800 N. Quincy Street
Arlington, VA 22217
ATTN: Code 102 IP

78 10 12 025

Unclassified

SECURITY CLASSIFICATION OF THIS PAGE (When Data Entered)

REPORT DOCUMENTATION PAGE		READ INSTRUCTIONS BEFORE COMPLETING FORM
1. REPORT NUMBER	2. GOVT ACCESSION NO.	3. RECIPIENT'S CATALOG NUMBER
4. TITLE (and Subtitle) A NOVEL CONCEPT FOR A SELF-FOCUSING AND TARGET SEEKING SONAR SYSTEM		5. TYPE OF REPORT & PERIOD COVERED Final Report, March 75-May 78
6. AUTHOR(s) DR Rolf K. Mueller		7. PERFORMING ORG. REPORT NUMBER
8. PERFORMING ORGANIZATION NAME AND ADDRESS University of Minnesota Electrical Engineering Dept. Minneapolis, Minnesota 55455		9. CONTRACT OR GRANT NUMBER(s) N00014-75-C-0631
10. CONTROLLING OFFICE NAME AND ADDRESS Office of Naval Research (Code 222) 800 N. Quincy St. Arlington, Va 22217		11. PROGRAM ELEMENT, PROJECT, TASK AREA & WORK UNIT NUMBERS 62711N, RF11-121, RF11-121-801, NR261-201
12. MONITORING AGENCY NAME & ADDRESS (if different from Controlling Office)		13. REPORT DATE 16 May 78
		14. NUMBER OF PAGES 77
		15. SECURITY CLASS. (of this report) Unclassified
		16a. DECLASSIFICATION/DOWNGRADING SCHEDULE NA
16. DISTRIBUTION STATEMENT (of this Report) Approved for public release; distribution unlimited.		
17. DISTRIBUTION STATEMENT (of the abstract entered in Block 20, if different from Report) 12 81 p. 16 F111121 17 RF111121801		
18. SUPPLEMENTARY NOTES		
19. KEY WORDS (Continue on reverse side if necessary and identify by block number) Acoustics, Self-Focusing Array, Retrodirective Targeting		
20. ABSTRACT (Continue on reverse side if necessary and identify by block number) A new concept for a retrodirective target-seeking sonar system is described. The system is based on time reversal. This is achieved by storing the target return in a serial access memory and reading out the stored information in reverse order for retransmission. 2.33 52.0 "Continued on back side"		

DD FORM 1 JAN 73 1473

EDITION OF 1 NOV 65 IS OBSOLETE
S/N 0102-LF-014-6601

Unclassified

SECURITY CLASSIFICATION OF THIS PAGE (When Data Entered)

Unclassified

SECURITY CLASSIFICATION OF THIS PAGE (When Data Entered)

Continued from Block 20

→ The theory of the device is given for noise-free operations and stationary array and targets. The motion sensitivity of the system is discussed and the effect of white noise and reverberation noise on the system considered. A computer simulation of the system in a reverberation environment is described and some results of the simulation given. ↗

S/N 0102-LF-014-6601

Unclassified

SECURITY CLASSIFICATION OF THIS PAGE(When Data Entered)

Abstract

A new concept for a retrodirective target-seeking sonar system is described. The system is based on time reversal. This is achieved by storing the target return in a serial access memory and reading out the stored information in reverse order for retransmission.

The theory of the device is given for noise-free operations and stationary array and targets. The motion sensitivity of the system is discussed and the effect of white noise and reverberation noise on the system considered. A computer simulation of the system in a reverberation environment is described and some results of the simulation given.

ACCESSION for		
NTIS	White Section	<input checked="checked" type="checkbox"/>
DDC	Buff Section	<input type="checkbox"/>
UNANNOUNCED		<input type="checkbox"/>
JUSTIFICATION		
BY		
DISTRIBUTION/AVAILABILITY CODES		
Dist.	AVAIL.	and/or SPECIAL
A		

I. Introduction

The concept of retrodirective and target seeking radar or sonar systems is not new. In 1940 L. C. Van Atta received a patent¹ for a retrodirective phased array. It functions like a corner reflector sending impinging plane waves back into themselves. This retrodirectivity is achieved in both the corner reflector and the Van Atta array by inverting the space coordinates of the wave. In the Van Atta array the space inversion is done by connecting the receive array elements located at (x_n, y_n) to the corresponding space inverted elements $(-x_n, -y_n)$ of a transmit array.

If one puts amplifiers between the receive and transmit arrays the Van Atta array can be made target seeking. A self-seeking communication system based on this concept has been described in the literature.²

We shall in the following describe a system which is based on time inversion instead of space inversion. The time inversion system has a number of desirable characteristics which cannot be achieved with a Van Atta array. These characteristics include: self-focusing, partial motion compensation, target position independent echo return time and a tendency to prevent echoes from spreading out in time.

We shall discuss in this report possible implementations of such a system, its beamforming characteristics in a noise-free environment including

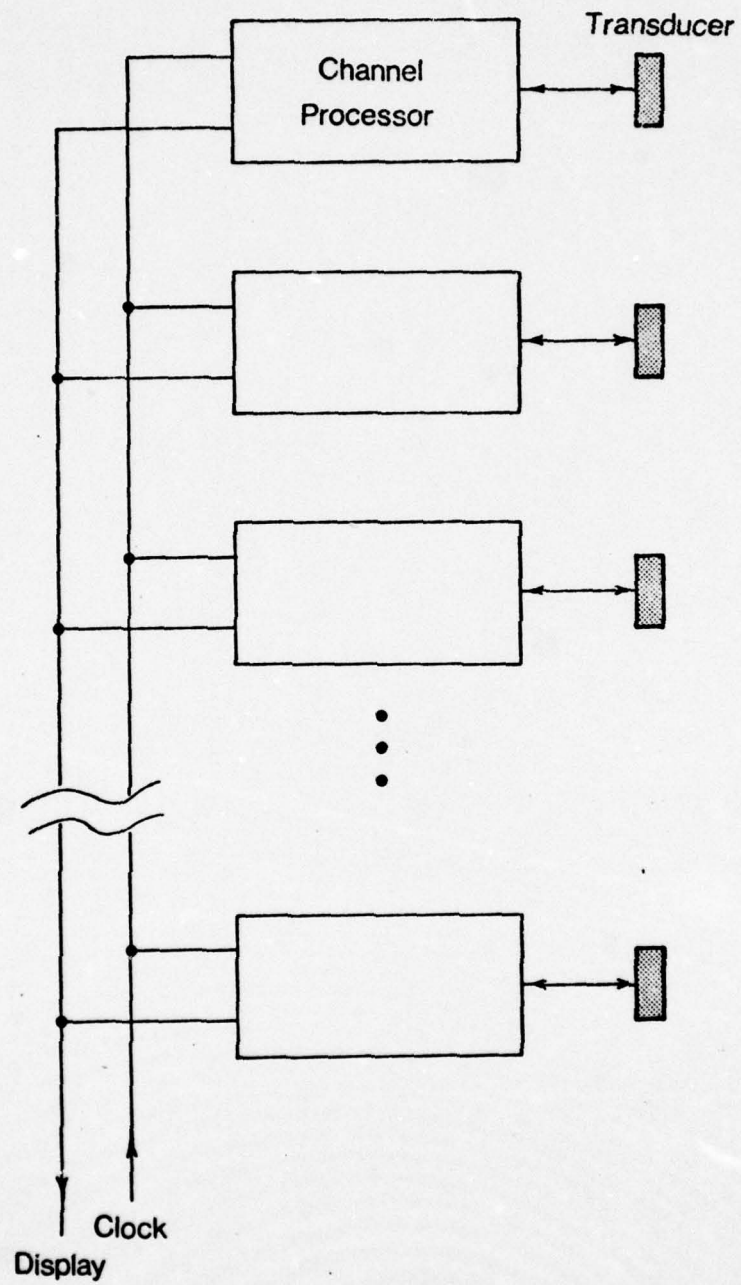


Fig. 1

motion sensitivity and configuration stability, the effect of signal independent white noise and the system performance in a reverberation environment.

II. The System

The concept of a time inversion retrodirective sonar (or radar) is straightforward; it is based on the fact that an outgoing spherical wave changes under time inversion into an incoming spherical wave converging toward its center. Therefore, if an array of transducers receives and stores over a period of time a signal or echo from a point source and retransmits the stored signal in reverse order, that is, inverted in time, a beam results which is focussed on the original source position. If more than one source is present in the field, retro-directive beams focussed on each one of the sources are generated. This characteristic makes the time inversion system potentially useful as a target seeking and tracking device. We describe in this section the basic components of such a system and give a brief summary of its operational characteristics.

Figure 1 shows a schematic of the system. It consists of an array of N transducers, each connected to its own channel processor. The processor-transducer combination is self-contained and the N units can be distributed arbitrarily in space, connected only by wire or radio link to a common clock and

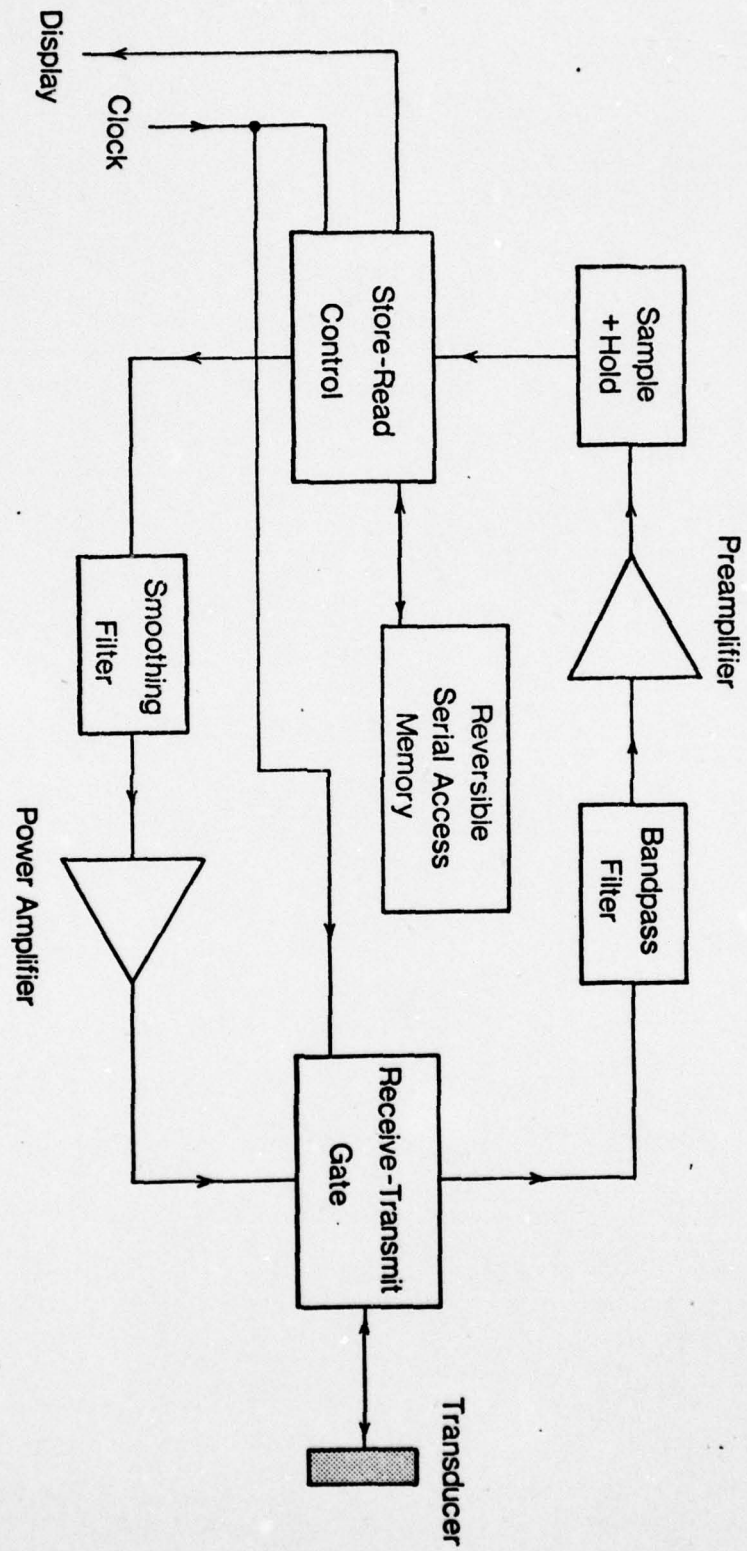


Fig. 2

display. In one possible implementation the central element of the array is connected to a search pulse generator. The target seeking process in this case is initiated by the emission of a search pulse by this central element. We shall use this model for our discussion of the system characteristics.

Figure 2 shows one transducer with its channel processor. A clock operates the transmit-receive gate, samples the data and controls their transport in and out of a serial access memory. In the receive mode the signal is amplified, sampled and clocked into a serial access memory. The "store-read gate" routes the data samples in and out of the memory and supplies appropriately coded information to a display unit which displays the content of the entire memory bank.

The system performance depends critically on the characteristics of the memory devices. The number N of stored samples which are necessary to adequately describe a signal of duration T and bandwidth B is according to the Nyquist sampling theorem:

$$N = 2BT \quad (1)$$

The signal duration T is directly related to the range R over which targets are being acquired by the system:

$$T = 2R/c \quad (2)$$

where c is the signal propagation velocity. The bandwidth B is similarly related to the range resolution ΔR :

$$B = c/2\Delta R \quad (3)$$

The maximum range R and the resolution ΔR of a time inversion system are limited by the retention time ΔT of the memory and the maximum clock rate ρ at which data samples can be moved.

Because of the time inversion the first signal sample clocked into the memory is the last one to be clocked out and, therefore, stays in the memory for a period of time equal to twice the signal return time T . We have, therefore, a limiting condition for the retention time ΔT :

$$\Delta T \geq 2T \quad (4)$$

and because of Equation (2) a limiting condition for the range R :

$$R \leq c\Delta T/4 \quad (5)$$

The minimum clock rate necessary to store an incoming signal of bandwidth B is:

$$\rho_{\min} = 2B \quad (6)$$

which gives together with equation (3) the limiting condition for the range resolution ΔR :

$$\Delta R = c/\rho \quad (7)$$

If we consider a typical high resolution sonar with a search range R of 500 meters and a range resolution ΔR of .1 meter, we find from the foregoing considerations the following requirements: A storage capacity of $N = 10^4$ bins, a minimum retention time of $T = 800$ msec and a clockrate of $\rho = 25$ kHz. These requirements have to be met together with a high dynamic

range and reversibility of the dataflow in a serial access memory. Presently available commercial charge coupled devices (CCD) or similar devices which satisfy the reversibility requirement almost meet these criteria. The most critical parameter is the retention time ΔT . Since the dynamic range of CCD's deteriorates with retention time and ambient temperature, the above time requirement can be met with presently available CCD's only if they are cooled. The required number N of storage bins is high but feasible, and the required clockrate orders of magnitude below device capability.

If we consider a search radar as a potential application and assume a range of 50 km and a range resolution of 10 meters we find that the same memory capacity of $N = 10^4$ storage bins is required, but a much smaller retention time of $T = .8$ msec and a minimum clockrate of $\rho \geq 30$ MHz. In this case the clockrate is the critical parameter but still within the capability of CCD's. The expected technical and economic feasibility of an adequate memory bank for a time inversion system in the near future makes it a timely task to analyze its characteristics.

III. The Array Target Interaction

In this section we derive the algebra which describes the interaction of the time inversion system with a field of targets.

We assume an array of K transducers and a field of J targets. The positions of the transducers and targets are described by position vectors in a cartesian coordinate system (x, y, z) which has its origin in one of the array elements, called the reference element. The reference element is the element closest to the center of gravity of the array. It is assumed that the radius r_{\min} of the smallest sphere which contains all array elements is small compared to the minimum distance R_{\min} from which targets are acquired by the system. The maximum distance from which targets are acquired is R_{\max} . The range R of operation of the system is $R = R_{\max} - R_{\min}$.

We limit the discussion in this section to a linear system, that is, we assume that the $n+1$ st retransmitted signal is a linear function of the n th target response which is in turn a linear function of the n th retransmitted signal. It is the purpose of this section to derive the linear operators which relate array output and target response to each other.

In order to avoid unnecessary complication we assume that the linear dimension 'a' of the individual transducers are of the order of the mean wavelength of the (bandlimited) search function. The farfield pressure wave generated by the k th element during the n th retransmission is, therefore, within a cone angle of $\theta = \sin^{-1}(\frac{\lambda}{a})$ a spherical wave $\frac{n_f^k(t-r/c)}{r}$. The characteristic function $n_f^k(t)$ of this spherical wave

has the dimension [Newton per meter] and is related to the voltage n_V^k across the k th transmitting transducer by

$$n_f^k = \alpha n_V^k \quad (8)$$

with the coefficient α given by

$$\alpha = \{(4a^2 \eta \rho c) / (\pi \lambda I)\}^{1/2} \quad (9)$$

where η is the efficiency of the electrical to mechanical energy conversion, ρ the density of the transmitting medium, and I the electrical impedance of the transducer.

We describe the total array output for the n th retransmission as the ordered set $n_F(t)$ of characteristic functions $n_{f_k}(t)$:

$$n_F(t) = \{n_{f_k}(t)\} \quad k = 0, \dots, K-1 \quad (10)$$

We assume further that the targets are "point scatterers" in the limited sense that they are small compared to the lateral resolution of the array. This implies that the backscattered wave is again adequately described by a spherical wave $n_{h_j}(t-r/c)/r$ within the small cone which the array subtends at the target. The target response function $n_H(t)$ is then again the ordered set of the generating functions $n_{h_j}(t)$ of these spherical waves:

$$n_H(t) = \{n_{h_j}(t)\} \quad j = 1 \dots J. \quad (11)$$

The limitation of our consideration to point targets does not limit the generality of our derivation since one can build up arbitrarily complex targets by an ensemble of suitably chosen point targets (Huyghens Principle).

It follows from the foregoing definitions that the pressure ${}^n p_j(t)$ at the j th target location due to the n th retransmission ${}^n F(t)$ is

$${}^n p_j(t) = \sum_k \frac{1}{r_{jk}} {}^n f_k(t - t_{jk}) \quad (12)$$

where r_{jk} is the distance between the j th target and the k th transducer and $t_{jk} = r_{jk}/c$ the corresponding propagation time. It is sufficient to approximate r_{jk} in the slow varying spreading term $1/r_{jk}$ by $r_j = r_{j0}$, the distance of the j th target from the array center.

We introduce the time delay operator $D(\tau)$ defined by

$$D(\tau)f(t) \equiv f(t - \tau) \quad (13)$$

and write equation (12) as:

$${}^n p_j(t) = \frac{1}{r_j} \sum_k D(t_{jk}) {}^n f_k(t) \quad (14)$$

The j th target response is a linear function of the pressure field at all target locations

$${}^n h_j(t) = \sum_{j'} S_{jj'} {}^n p_{j'}(t) \quad (15)$$

The ordered set $\{S_{jj'}\}$ is the scatter matrix of the target distribution. If we neglect multiple scattering the target response depends only on the primary pressure field ${}^n p_j(t)$ at its own location. The sum in equation (15), therefore, reduces to:

$${}^n h_j(t) = S_j(t) {}^n p_j(t) \equiv \sigma_j i_j(t) * {}^n p_j(t) \quad (16)$$

where σ_j is the backscatter cross section and $i_j(t)$ the normalized impulse response of the j th target.

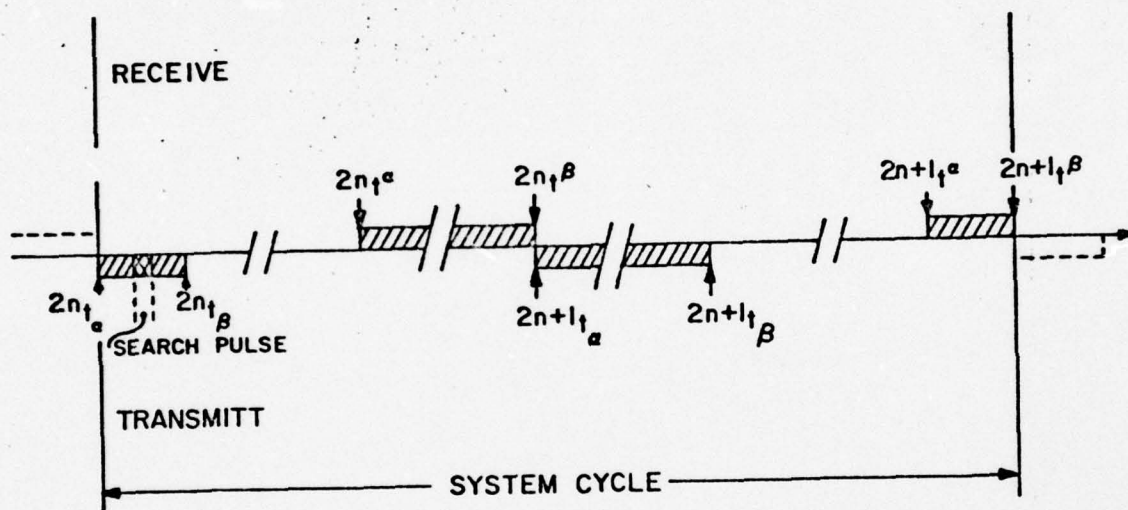


Fig. 3

The star in eq. (16) indicates convolution. Introducing equation (14) into equation (16) we obtain:

$$\begin{aligned} n_{h_j}(t) &= \sigma_j/r_j * \sum_k D(t_{jk}) n_{f_k}(t) = \\ &\sigma_j/r_j \sum_k D(t_{jk}) i_j(t) * n_{f_k}(t) \end{aligned} \quad (17)$$

To go to the right side of eq. (17) we made use of the commutability of the convolution operation with the time delay operator. This follows directly from the definition of the convolution operation:

$$g(t) * f(t) \equiv \int_{-\infty}^{+\infty} g(\tau) f(t-\tau) d\tau \quad (18)$$

We have shown above that in the neighborhood of the array the waves scattered back from the targets can be approximated by zero order spherical waves. We obtain, therefore, for the pressure $n_{p_k}(t)$ at the location of the k th transducer:

$$n_{p_k}(t) = \sum_j \frac{1}{r_j} n_{h_j}(t-t_{jk}) \quad (19)$$

The voltage $n_{v_k}(t)$ generated by the k th receiving transducer due to the pressure $n_{p_k}(t)$ is:

$$n_{v_k}(t) = \beta n_{p_k}(t) \quad (20)$$

where β is the transducer constant.

In order to determine the next retransmitted signal $n_{f_k}^{n+1}(t)$ we have to keep track of the appropriate receive and transmission times, which are shown schematically in Fig. 3. We label the time at which the n th receive period is activated as n_t^α and the time at which it ends as n_t^β . During the receive time

$n_t^\alpha < t < n_t^\beta$ the transducers generate the voltages $n_{v_k}(t)$ which are amplified, filtered, sampled and stored. At $t = n+1 t_\alpha = n_t^\beta$ the $n+1$ st transmit mode is activated. The stored signals are read out in reverse order, filtered, amplified by a large factor γ (power amplification) and fed to their respective transducers. The transmit voltage $n+1 v_k$ across the k th transducer becomes:

$$n+1 v_k(t) = \gamma n_{v_k} \{ n_t^\beta - (t - n_t^\beta) \} \quad (21)$$

and the retransmitted signal $n+1 f_k(t)$ according to eq. (8)

$$n+1 f_k(t) = \alpha n+1 v_k(t) \quad (22)$$

The retransmission ends when all of the stored signal is retransmitted that is at time:

$$t = n+1 t_\beta = n+1 t_\alpha + (n_t^\beta - n_t^\alpha) = 2 n_t^\beta - n_t^\alpha \quad (23)$$

Combining equations (19) through (22) we obtain:

$$n+1 f_k(t) = D(2 n_t^\beta) \sum_j \frac{\kappa}{r_j} D(t_{jk}) n_{h_j}(-t) \quad (24)$$

where

$$\kappa = \alpha \beta \gamma \quad (24a)$$

Equations (17) and (24) are sufficient to relate the $n+1$ st retransmitted signal back to the original search pulse.

We assume for the following analysis that the initial pulse is transmitted by a single projector at the location of the array-element $k = 0$. The transmit gate opens at $t = {}^0 t_\alpha$ and closes at ${}^0 t_\beta$. In order to accommodate all later even retransmissions we let:

$${}^0 t_\beta - {}^0 t_\alpha = 2 n t_\beta - 2 n t_\alpha = 2 r_{\min}/c + \tau \quad (25)$$

where r_{\min} is the radius of the smallest sphere capable of enclosing the array and τ the pulse duration. The transmit time given by eq. (25) is the minimum time required to allow beamforming in any desired direction with all array elements participating. The projector which is in the center of the array in our model transmits during the time ${}^0t_\alpha + r_{\min}/c - \tau/2 < t < {}^0t_\alpha + r_{\min}/c + \tau/2$.

The target response to the initial search pulse ${}^0f(t)$ is according to equation (16)

$${}^0h_j(t) = \frac{\sigma_j}{r_j} D(t_{j0}) i_j * f(t) \quad (26)$$

In order to receive at all transducer locations the backscattered signal from all potential targets in the acquisition range R , it is necessary for the receive mode to begin at:

$$t = {}^0t^\alpha = 2(R_{\min} - r_{\min})/c + {}^0t_\alpha \quad (27a)$$

and to run until:

$$t = {}^0t^\alpha = 2(R_{\min} - r_{\min})/c + {}^0t_\alpha = \frac{2}{c}(R_{\max} + 2r_{\min}) + 2\tau + {}^0t_\alpha \quad (27b)$$

All potential target returns from within the acceptance range R of the system are now received; the array can, therefore, begin retransmission immediately. Labeling the beginning of the first retransmission ${}^1t_\alpha$ we have: ${}^1t_\alpha = {}^0t^\beta$. The transmission cycle runs until stored information is retransmitted, that is, until

$$t = {}^1t_\beta = 2{}^0t_\beta - {}^0t_\alpha = \frac{2}{c}(2R_{\max} - R_{\min} + 5r_{\min}) + 4\tau + t_\alpha \quad (28)$$

The first retransmitted signal $l_{f_k}(t)$ is obtained by introducing equation (26) into equation (24):

$$l_{f_k}(t) = D(2 \cdot t^\beta) \sum_{j=1}^J \frac{\kappa \sigma_j D(t_j - t_{jk})}{(r_j)^2} i_j(-t) * f(-t) \quad (29)$$

The target response $l_{h_j}(t)$ to that excitation follows if we introduce equation (29) into equation (17). After some rearrangement of the resulting double sum we obtain:

$$l_{h_j}(t) = \frac{\kappa \sigma_j D(2 \cdot t^\beta)}{r_j} \sum_k \sum_{j'} \frac{\sigma_{j'}}{(r_{j'})^2} D(t_{jk} - t_{j'k} - t_{j'}) i_j(t) * i_{j'}(-t) \times f(t) \quad (30)$$

We note that the term with $j' = j$ in the sum over j' in eq. (30) corresponds to the excitation of the j th target by its own retrodirected beam. The contributions from all k transducers become equal and add coherently. The terms with $j' \neq j$ are the side lobe contributions at the j th target from beams focussed at the other targets. To set this in evidence we rewrite equation (30) to read:

$$l_{h_j}(t) = D(2 \cdot t^\beta) \cdot \left\{ \frac{\kappa K \sigma_j^2}{(r_j)^3} D(-t_j) a_j(t) * f(-t) + \sum_k \sum_{j' \neq j} \frac{D(t_{jk} - t_{j'k} - t_{j'}) \kappa_j \sigma_{j'}}{r_j^2 r_{j'}} \cdot c_{jj'}(t) * f(-t) \right\} \quad (31)$$

where $a_j(t)$ is the autocorrelation function of the target impulse response:

$$a_j(t) = i_j(t) * i_j(-t) \quad (32)$$

and $c_{jj'}(t)$ the cross correlation between the impulse responses of the j th and j' th target:

$$c_{jj'}(t) = i_j(t) * i_{j'}(-t) \quad (33)$$

The side lobe contributions to $l_h(t)$ given by the double sum in equation (31) are in general very small compared to the focussed beam contributions given by the first term in eq. (31). This is true firstly because the side lobe level of pulsed systems is already low and secondly because the cross correlation functions $c_{jj'}$ of the impulse responses of different targets can be expected to be small compared to their autocorrelation functions. However, another very effective side lobe reduction specific to the present system is possible through appropriate timing of the receive period during which the back-scattered signal $l_{h_j}(t)$ is accepted.

The pressure field $l_{p_k}(t)$ at the array due to $l_{h_j}(t)$ follows from eqs. (19) and (31):

$$l_{p_k}(t) = D(2 \circ t^\beta) \left\{ \sum_j \frac{\kappa \sigma_j^{2K}}{(r_j)^4} D(t_{jk} - t_j) a_j(t) * f(-t) + \right. \\ \left. + \sum_k \sum_{j' \neq j} \frac{\kappa \sigma_j \sigma_{j'}}{(r_j)^2 (r_{j'})^2} D(t_{jk'} + t_{jk} - t_{j'k'} - t_{j'}) c_{jj'}(t) * f(-t) \right\} \quad (34)$$

Equation (31) shows that the main lobe contributions from all targets arrive at the reference element ($k=0$) at the same time $t = 2 \circ t^\beta$. If the targets are point targets the autocorrelation functions $a_j(t)$ are delta functions and the backscattered field seen by

the array elements is proportional to the search pulse (inverted in time). Due to the finite extension of the array, the first signal at any array element arrives at

$$t \geq 2 \cdot t^\beta - r_{\min}/c$$

and has passed the array at $t \leq 2 \cdot t^\beta + r_{\min}/c + \tau$.

If one, therefore, sets the receive gate to open at:

$$1_{t^\alpha} = 2 \cdot t^\beta - r_{\min}/c = \frac{4}{c} R_{\max} + \frac{4}{c} r_{\min} + 4\tau + t_\alpha \quad (35)$$

and close at:

$$t = 1_{t^\beta} = 2 \cdot t^\beta = 2 \cdot t^\beta + \frac{r_{\min}}{c} + \tau = \frac{4}{c} R_{\max} + g/c + r_{\min} + 5\tau + t_\alpha$$

all main lobe signal returns will be received. For extended targets for which the autocorrelation functions $a_j(t)$ are not delta functions, but by definition symmetrical functions with a maximum at $t = 0$, the same receive gate setting still assures the reception of a major portion of the main lobe return signals from all targets.

The short duration of the receive mode ($1_{t^\beta} - 1_{t^\alpha} = \tau + \frac{2r_{\min}}{c}$) excludes most side lobe returns.

They are accepted only from target pairs with a range difference $r_{jj'}$, of the order of the linear array dimension:

$$r_{jj'} \leq 4r_{\min} + \tau c \quad (36)$$

Equation (27a,b) and (28) assure that the beginning of the receive mode 1_{t^α} is compatible with the end 1_{t^β} of the previous transmit mode.

After all main lobe returns are received, the system is ready for the next transmission period which starts at $t = {}^2t_\alpha = {}^1t_\beta$. The retransmission lasts till all stored signals are retransmitted, that is, until:

$$t = {}^2t_\beta = {}^2t_\alpha + {}^1t_\beta - {}^1t_\alpha = {}^2t_\beta - {}^1t_\alpha.$$

The retransmitted signal ${}^2f_k(t)$ now follows from eqs. (31) and (24):

$${}^2f_k(t) = D({}^2t_\beta) \sum_j \frac{\kappa^2 \sigma_j^2 K}{(r_j)^4} D(t_j - t_{jk}) a_j(t) * f(t) + \text{side lobe terms.} \quad (37)$$

The side lobe terms are small and almost always gated out. We shall, therefore, neglect them from here on. Note that the autocorrelation function $a(t)$ is not affected by time reversal since it is by definition a symmetric function. The time delay factor $D({}^2t_\beta)$ in front of the sum can be deleted if we introduce a new time reference:

$$t' = t - {}^2t_\beta \quad (38)$$

and write the running time again as t instead of t' . Equation (37) implies that the total array output for the second retransmission represents J beams focused back onto the J targets. This insonification generates the target response ${}^2h_j(t)$ which we obtain by substituting eq. (37) into eq. (17) again neglecting all side lobe terms:

$${}^2h_j(t) = \frac{g_j^2 \sigma_j^2 D(t_j)}{r_j} a_j(t) * i_j(t) * f(t) \quad (39)$$

with

$$g_j = \frac{\kappa K \sigma_j}{r_j^2} \quad (39a)$$

If one compares ${}^2h_j(t)$ given by eq. (39) with the target response ${}^0h_j(t)$ due to the initial search pulse which is given in eq. (26) one obtains:

$${}^2h_j(t) = g_j {}^2a_j(t) * {}^0h_j(t) \quad (40)$$

The autocorrelation function $a_j(t)$ of the target impulse response is, up to a scale factor, a δ -function for point targets or a narrow pulse like function for complex extended targets. Therefore, eq. (40) implies that the second (and, therefore, all even) iterations of the target response are more or less perfect replicas of the target response to the initial search pulse:

$${}^{2n}h_j(t) = g_j^2 \cdot a_j(t) * {}^{2(n-1)}h_j(t) = g_j^{2n} a_{jn}(t) * {}^0h_j(t) \quad (41)$$

where a_{jn} is the n -th iteration of the $a_j(t)$:

$$a_{jn}(t) = a_j(t) * a_j(t) \dots * a_j(t) \quad (42)$$

Since the n -th target output ${}^nf_k(t)$ is a linear function of the $(n-1)^{st}$ target response, the quasi-periodicity of nh_j carries over to ${}^nf_k(t)$:

$${}^{2n}f_k(t) = \sum_j \frac{g_j^{2n} D(-t_{kj})}{K} a_{jn}(t) * f(t) \quad (43)$$

and

$${}^{2n+1}f_k(t) = \sum_j \frac{g_j^{2n+1}}{K} D(t_{kj}-t_j) \sigma_j(-t) * a_{jn}(t) * f(-t) \quad (44)$$

If the round-trip gain factor g_j equation (43) is greater than unity the array output increases with every iteration (equation 43,44). If the round-trip gain factor for a given target is smaller than unity then the target insonification dies out. Since g is

proportional to the scatter cross section and inversely proportional to the target distance, a free-running system singles out the strongest and closest targets. If the output signal amplitude is limited, the system tends to automatically equalize the beam strength for each target beam provided g_j is greater than unity.

Equations (43) and (44) show two significant differences between the even and odd retransmission functions. The even retransmission represents j simultaneously transmitted beams focused on the j targets. The waveform on each beam is practically identical, consisting of a more or less true replica of the waveform of the search pulse. In contrast the odd retransmissions represent j beams which are spaced out in time and which have target specific waveforms. The waveforms are essentially the initial pulse convolved with the respective target impulse response. They preserve, therefore, the target signature. The emission time of each beam is proportional to the range of its target. This is a useful feature since it permits one to select one or more particular targets by simply gating out the corresponding beams. This gating has to be done only once; from there on the system continues to track only the selected targets.

We arrived at the relatively simple results of eqs. (43) and (44) by neglecting all side lobe

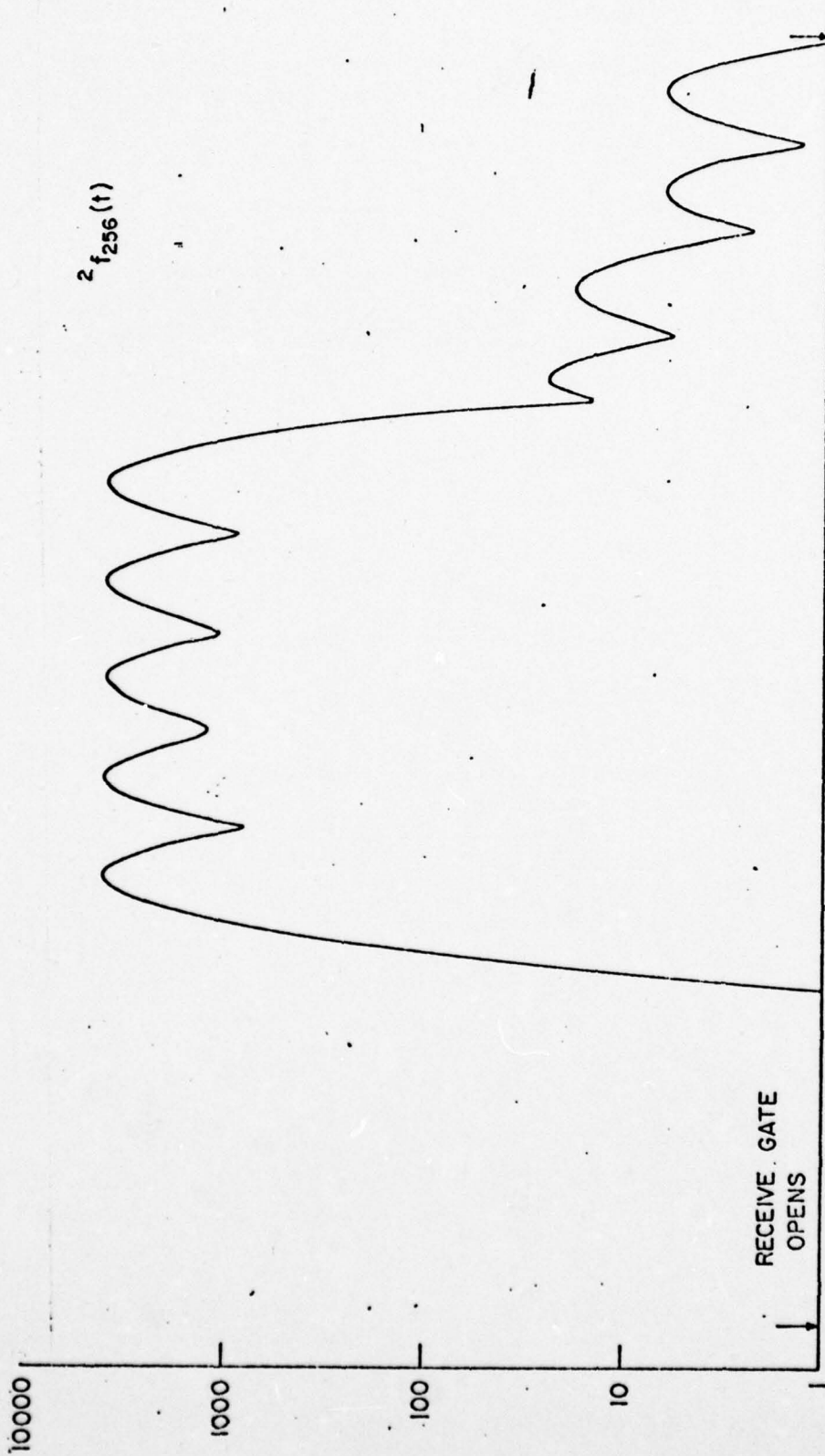


Fig. 4

contributions. To verify the validity of this approximation, a computer model of the system including all side lobe contributions was developed. The program is given in Appendix I. Some results of the model study are shown in Figs. 4 and 5. The following model was used to obtain this result: The transmit receive unit of the system was a linear array of 513 equally spaced elements with $d = \lambda/2$. The center element was at $k = 0$. It emitted the initial search pulse $\phi(t)$. The search pulse was chosen to be a single-frequency pulse with a gaussian envelope:

$$\phi(t) = e^{-i2\pi\nu t} e^{-\left(\frac{\nu t}{5}\right)^2}$$

The system operated against a field of 5 point targets of equal cross section. The location of the targets is shown in Table 1.

Table 1

Target	$x/10^3\lambda$	$z/10^3\lambda$
1	-6	20
2	-2	20
3	0	20
4	+2	20
5	+6	20

Target Locations

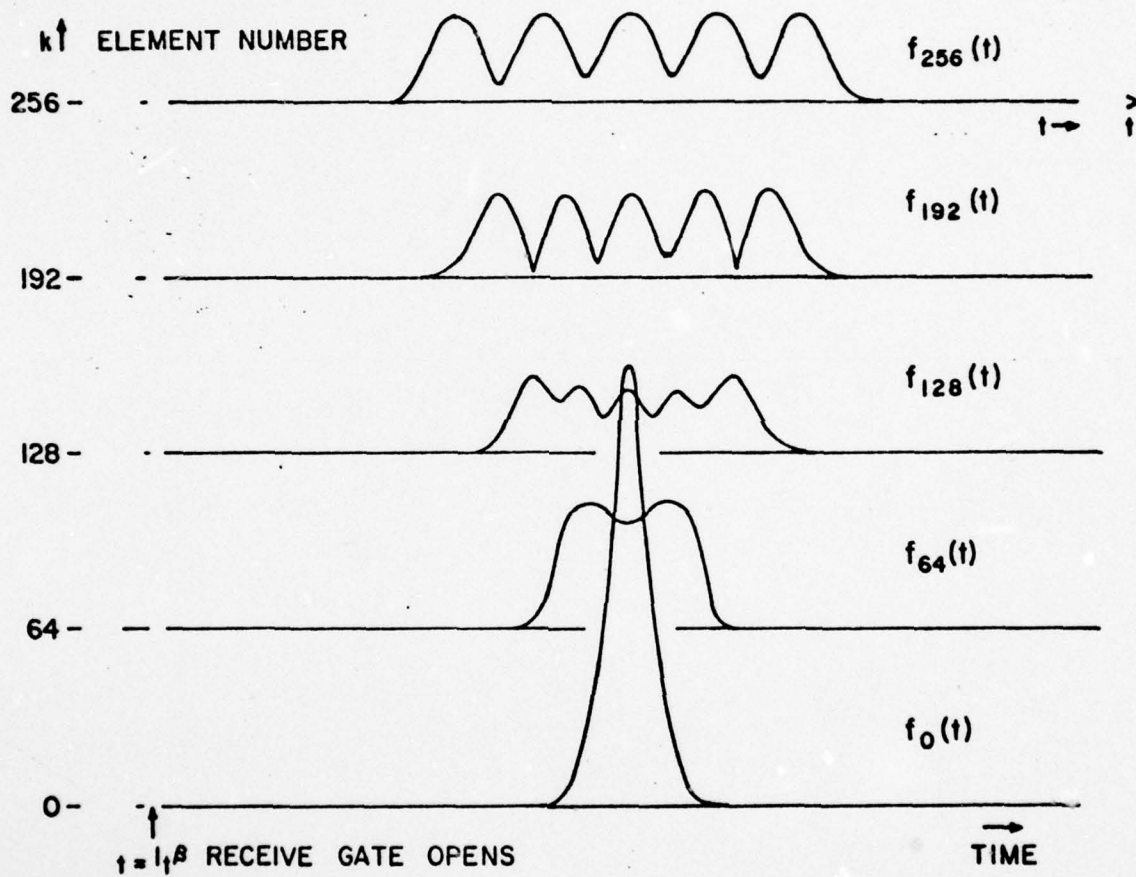


Fig. 5

The target positions were chosen symmetrically around the z axis to assure that side lobe contributions were received during the short receive period $\Delta t = (t_\beta - t_\alpha)$. Figure 6 shows the envelope of the output voltage $v_k(t)$ eq. (24) of the receiving array elements during Δt for the element $k = 256$ on a logarithmic scale which puts the side-lobe contributions in evidence. Note that the side-lobe contributions are two orders of magnitude smaller than the main returns. Figure 7 shows the returns of elements 256, 192, 128, 69, and 0 on a linear scale. The side-lobe effects are no longer visible. The beamforming delays between channels can be clearly seen.

IV. Motion Sensitivity

The time inversion systems described above focus the energy of each successive ping back to the area where the previous ping encountered a target. The effect of this self-focusing is to enhance the target insonification in successive pings over that obtainable with a non-directional system. This objective, however, can be reached only if the target has not moved out of the focal area during the time between pings. Since the linear dimension of the focal area is inversely proportional to the aperture of the array, this motion sensitivity imposes a limit to the useful aperture of a system operating against moving targets. Since the lateral extent of the focal

area is smaller than the depth of focus, the critical target motion is the motion perpendicular to the line connecting the target with the array. In order to find the maximum aperture size which can be used effectively against moving targets, we need to consider only this worst case. If the time between pings is Δt and the target velocity is v , the distance travelled between pings by the target is

$$d = \Delta t \cdot v \quad (45)$$

This distance has to be compared with the halfwidth of the focal area F :

$$F = \frac{R_j \lambda}{D} \quad (46)$$

where λ is the wavelength of the center frequency of the search pulse and D the effective diameter of the array aperture. Since by design the target starts out in the center of the focal area, the travelled distance d between pings must be not greater than $1/2 F$. The limiting condition for the array aperture, therefore, becomes:

$$d \leq \frac{\lambda R_j}{2D} \quad (47)$$

or

$$D \leq D_c = \frac{\lambda R_j}{2d} = \frac{\lambda R_j}{2\Delta t \cdot v} \quad (48)$$

where D_c is the critical aperture. We have seen above that the time between pings in our system depends on whether the last ping was due to an odd or even retransmission. Referring to Fig. (3) and eq. (27b) we find:

$$c \cdot \Delta t_{\text{odd}} = 2n_t \beta - 2n_t \alpha + 2R_{\text{max}} - 2R_j = 4R_{\text{max}} - 2R_j \quad (49)$$

Equation (49) shows that for odd retransmission the elapsed time between the present and the previous ping is largest for targets close to the array.

This is due to the fact that the returns from nearby targets spend extra time in the system memory. The elapsed time for even retransmissions is simply:

$$c \cdot \Delta t_{\text{even}} = 2^{n+1} t^{\beta} - 2^{n+1} t^{\alpha} - 2R_{\text{max}} + 2R_j \approx 2R_j \quad (50)$$

which is for all targets smaller than Δt_{odd} of eq. (49). Since the system has to accommodate the largest elapsed time $(\Delta t_{\text{odd}})_{\text{max}}$:

$$c \cdot (\Delta t_{\text{odd}})_{\text{max}} = 4R_{\text{max}} - 2R_{\text{min}} = 2(2R + R_{\text{min}})$$

we obtain for the critical aperture D_c of eq. (48):

$$D_c = \frac{\lambda c R_{\text{min}}}{4v(2R + R_{\text{min}})} \quad (51)$$

The severity of the aperture limitation given by eq. (51) depends on the factor c/v . In the radar case where the factor c/v for target speeds of interest is very large the critical aperture D_c is much larger than the aperture size required for a practical system. For target velocities of Mach 10 the factor c/v is still about 10^5 and D_c , therefore, of the order of $10^4 \lambda$.

The situation is quite different in the sonar case. Here c/v for targets with a velocity of 50 km/h is only about 10^2 and the critical aperture, therefore, of the order of a few wavelengths, which is too small for a practical search and tracking sonar. We shall discuss in the next section a simple system modification which partially overcomes this difficulty.

System Modification for Tracking Moving Targets

The critical aperture D_c equation (51) is required to assure proper insonification of all targets during all retransmissions. The limit is imposed by the odd retransmissions and within the odd retransmissions by the targets closest to the array.

For even retransmissions the permissible aperture \bar{D} is independent of the target range and equal to:

$$\bar{D} = d/(c \cdot \Delta t_{\text{even}}) = \lambda c/2v \quad (52)$$

The aperture required to properly insonify the most distant target during odd transmissions is equal to \bar{D} since for $R_j = R_{\text{max}}$ the time lapse Δt_{odd} becomes equal to Δt_{even} :

$$c \cdot \Delta t_{\text{odd}} = 2(2R_{\text{max}} - R_j) = 2R_j = c \cdot \Delta t_{\text{even}} \text{ for } R_j = R_{\text{max}}. \quad (53)$$

One can, therefore, satisfy the insonification requirement for distant targets by starting out the odd retransmit period with the full aperture \bar{D} (which is greater than D_c by a factor $(2 + \frac{4R}{R_{\text{min}}})$ and reduce the aperture linearly with time to reach D_c at the end of the odd retransmit period. The full aperture \bar{D} is used for the even retransmits. This modification can be made simply by adjusting the transmit gates for the different array element such that toward the end of the odd transmit period only a central portion of the array is left to transmit.

The net effect of this system modification is that the diameter at focus for all beams is commensurate with the maximum distance travelled by the generating target.

The most severe loss in angular resolution and beam intensity occurs for targets closest to the transmitting array, that is, for the case where it is least detrimental since for the closest target the aspect angle is largest and the spreading loss of the beam a minimum.

In spite of the improvement by a factor $(2 + \frac{4R}{R_{\min}})$ the new maximum aperture \bar{D} is still relatively small and represents for sonar applications a practical system limitation. For target velocities up to 50 km/h, for example, the maximum useful aperture is still only 50λ .

We shall show in the following section that this aperture limitation can be removed completely for a system which operates from a moving platform against a field of stationary targets.

Moving Array Stationary Targets

We consider in this section the practically important case of an array mounted on a moving platform operating against a field of stationary targets. A mine hunting sonar is an example of such a system. We shall show that a minor system modification removes in this case all aperture limitation.

The aperture limitation discussed above guaranteed that the radius at focus of each beam was larger than the maximum distance a target could travel between pings. This is necessary because in this system the retrodirected beam is focussed on the spot where the last ping encountered a target. In the moving platform situations, one can use the knowledge of the platform velocity to partially compensate for the apparent target motion by advancing appropriately the focal point of the retrodirected beam.

We consider first the even retransmissions. Complete time reversal would require that the platform moves during the transmission period backwards along the same path it moved during the receive period. The re-emitted beam would then focus exactly on the target location. One can simulate the effect of the reverse platform motion on the transmitted wave by slowing down by a factor $(1-2v/c)$ the clock rate which controls the data readout during retransmission. The factor $(1-2v/c)$ contains twice the doppler correction v/c . This comes about since we want to simulate reverse motion on a platform which continues to move forward. The retransmitted beam is now focussed back onto the target with the focal point displaced only by the small distance $\Delta = (2^n t^\beta - 2^{n-1} t_\alpha) v$, which the platform has moved between the beginning of the reception and the end of transmission periods. The displacement Δ is of the order of $D \cdot v/c$, that is, even for

the closest targets small compared to the focal diameter $\frac{\lambda R_{\min}}{D}$. In other words we can for the even transmission keep the target in focus by slowing down the transmission clock rate by the factor $(1-2v/c)$. The same argument holds for odd retransmissions if the target is at the end of the range $R_j = R_{\max}$. The changing aperture approach discussed in the previous section, therefore, applies also to the moving platform. No restrictions on the maximum aperture are now necessary. The only requirement is to make the clock rate for all retransmissions smaller by a factor $(1-2v/c)$ than that for receptions.

Internal Array Motion for Non-rigid Arrays

If the array consists of independent units as suggested in Section 2 (deployed, for example, as sonobouys), the most critical motion affecting the operation of the system is the displacement of the array elements against each other during the receive-transmit times. These time intervals are, as we have seen earlier in Section II, orders of magnitude different for the odd and even receive-transmit periods.

$$\begin{aligned}\Delta t_{\text{even}} &= (2n_t \beta - 2n-1 t_\alpha) \approx 4r_{\min}/c + \tau \approx 2D/c \\ \Delta t_{\text{odd}} &= (2n+1 t_\beta - 2n t_\alpha) \approx 4R/c\end{aligned}\tag{54}$$

Δt_{odd} is of the order of seconds; Δt_{even} is of the order of milliseconds. The permissible relative displacement of array elements between reception and retransmission is a fraction of a wavelength for

coherent signal addition at the target. This condition is not generally satisfied for the long time interval Δt_{odd} . One rather has to expect that for higher resolution sonars the array element position is a random variable with a variance approaching or exceeding a wavelength. For the short time interval Δt_{even} , however, one can assume that coherence between received and transmitted beam is maintained.

This implies that for odd retransmissions the intensities of the various array element contributions add up at the targets, whereas for even retransmission the amplitudes add coherently at the target to give the full array gain. We have shown earlier that the round-trip gain factor g defined in equation (40) is a useful parameter to describe the system performance. The round-trip gain factor g_e for the coherent, even retransmissions is equal to the round-trip gain g given in eq. (40); for the incoherent, odd retransmission the round-trip gain factor g_{odd} becomes due to the addition of intensities, rather than amplitudes, approximately equal to:

$$g_{\text{odd}} = g/\sqrt{K} \quad (55)$$

The average gain factor \bar{g} for a full cycle of even and odd retransmissions for the non-rigid array is therefore:

$$\bar{g}^2 = g_e \cdot g_o = g^2/\sqrt{K} \quad (56)$$

Since the gain factor for the rigid array is proportional to eq. (40), the average gain factor \bar{g} for the free-floating array is proportional to $K^{3/4}$. This implies, for example, that a non-rigid array of 500 elements has about the same average array gain as a rigid array of 100 elements.

Such a system makes very inefficient use of its data storage capability. It stores like a rigid array system in every memory element the complete signal sequence received during the long even receive period. In a stationary array this serves to generate the coherent and focused odd insonification beams which carry not only the spatial (angular and focus) information but also the temporal (high resolution) range information. The spatial information is rendered useless by the randomization of the element positions and the temporal information is highly redundant since it appears in all element memories essentially unchanged. One can argue that the spatial information is used to form the incoherently focused beams and are not really rendered useless. However, the total power at the target is only K times the power of each individual element contribution. One could, therefore, achieve the same power level at the target by irradiating it with a single wide angle projector capable of emitting K times the power of an individual array element.

A possible system realization would be to use the reference element as driver for a powerful projector activated for the odd retransmissions. The reference element alone would be equipped with a high-capacity memory of $n=2\Delta t_e/\tau$ bins which acquires the range information for the targets in the field.

V. White Noise

We discuss in this section the response of the system to additive white noise, that is, to thermal noise at the input of the preamplifiers of each channel. We assume that the noise power P and all other pertinent circuit parameters are identical in all channels. The noise added to the amplified and filtered signal which is read into the channel memory during each receive period is $\sqrt{P} \, {}^m n_k(t)$ where \sqrt{P} is the RMS noise voltage and ${}^m n_k(t)$ a normalized band-limited noise process. The superscript m refers to the m th receive period, the subscript k to the k th channel. The processes ${}^m n_k(t)$ are statistically independent for different m and k with a covariance Matrix:

$${}^{mm'} R_{kk}, \{t, (t+\tau)\} = \delta_{mm'} \delta_{kk'} a(\tau) \quad (57)$$

where $a(\tau)$ is the autocorrelation function of the impulse response of the filter following the preamplifier in each channel (see Fig. 2). The δ are the Kronecker δ :

$$\delta_{\alpha\beta} = \begin{cases} 1 & \text{for } \alpha = \beta \\ 0 & \text{otherwise} \end{cases} \quad (58)$$

We have assumed a linear system. We can, therefore, without loss of generality, consider the response of the system to the noise input only and later add this noise response to the response of the system to a search pulse of which we considered in section I.

We assume that the memory for each element contains a sample $^{\circ}n_k(t)$ of the noise function. At $t = ^{\circ}t_{\alpha}$ the transmit mode is enabled and the array transmits the function:

$$^{\circ}f_k(t) = \sqrt{P} ^{\circ}n_k(-t) \text{rect}_0(t) \quad (59)$$

where $\text{rect}_0(t)$ is the rectangular pulse:

$$\text{rect}_0(t) = \begin{cases} 1 & \text{for } ^{\circ}t_{\alpha} \leq t \leq ^{\circ}t_{\beta} \\ 0 & \text{otherwise} \end{cases} \quad (60)$$

The target response at the j th target is according to eq. (17) for point targets

$$^{\circ}h_j = \frac{\sigma_j \sqrt{P}}{r_j} \sum_k D(t_{jk}) ^{\circ}n_k(-t) \text{rect}_0(t) = \frac{\sigma_j \sqrt{PK}}{r_j} D(t_j) ^{\circ}n_j(t) \quad (61)$$

where

$$^{\circ}n_j(t) = \frac{1}{\sqrt{K}} \sum_k (D(t_{jk} - t_j) ^{\circ}n_k(-t) \cdot \text{rect}_0(t)) \quad (62)$$

The function $^{\circ}n_j(t)$ is again a normalized noise function.

The backscattered signal at the array due to the target response $^{\circ}h_j$ given by eq. (61) is in view of eq. (19)-(21)

$$l_{v_k}(t) = \beta \gamma \sqrt{PK} \sum_j \frac{\sigma_j}{r_j^2} D(t_j + t_{jk}) n_j(t) \quad (63)$$

In order to avoid unnecessary complications we assume that the target ranges r_j are sufficiently different so that the backscattered signals from different targets do not overlap in time. At $t = {}^0t^\alpha$ the receive gate is activated. The signal $l_{v_k}(t)$ is generated by each element and a new noise sample $n_k(t)$ is added. The combined received signal and noise is amplified, filtered and read into the memory. At $t = {}^0t^\beta = t_\alpha$ the transmit mode is activated. The memory content is clocked out in reverse order and the system generates the first retransmitted output $l_{f_k}(t)$ which is according to eqs. (22), (39a) and (63):

$$l_{f_k}(t) = \sqrt{\frac{P}{K}} \sum_j g_j D(-t_j - t_{jk}) {}^0n_j(-t) + \sqrt{P} D(-{}^0t^\beta) l_{n_k}(-t) \quad (64)$$

The first term on the right side of equation (64) represents the J retrodirected beams generated from the backscattered target excitation 0h_j given by eq. (61). The second term is due to the noise added to the received signal.

In order to evaluate the relative significance of the two contributions to the retransmitted signal l_{f_k} , we consider the resulting target excitation $l_{p_j}(t)$. Neglecting the side lobe contributions as irrelevant, we obtain for $l_{p_j}(t)$ according to eqs. (14) and (64):

$${}^1p_j(t) = \sqrt{PK} g_j D(-t_j) {}^0n_j(-t) + \sqrt{PK} D(-t^{1\beta}) {}^1n_j(t) \quad (65)$$

where ${}^1n_j(t)$ is again a normalized noise function defined analogous to 0n_j in equation (62) as

$${}^1n_j(t) = \frac{1}{\sqrt{K}} \sum_k (Dt_{jk} - t_j) {}^1n_k(-t) \text{rect}_1(t) \quad (66)$$

with

$$\text{rect}_1(t) = \begin{cases} 1 & \text{for } {}^1t_\alpha \leq t \leq {}^1t_\beta \\ 0 & \text{otherwise} \end{cases} \quad (67)$$

The two normalized noise functions 0n_j and 1n_j are uncorrelated. We have to compare, therefore, the intensities of the two contributions to the target excitation given by equation (65). We find that the intensity of the first term representing the retrodirected beam is $(g_j)^2$ times the intensity of the second term. g_j is the round-trip gain factor defined in equation (39a).

We shall now discuss the significance of this result in more detail. First we observe that the ratio z between the intensities of the backscattered and newly added noise at the transmitting array is, as follows from eq. (64):

$$z = (g_j)^2 / K \quad (68)$$

whereas at the target the corresponding ratio is according to eq. (65):

$$z_j = (g_j)^2 \quad (69)$$

The ratio $z_j/z = K$ is the array gain due to the coherent superpositions at the target of the retransmitted backscattered noise. The system has transformed this noise into a beamforming signal ${}^1s_k(t)$:

$$^1s_k(t) = \frac{\sqrt{P}}{K} \sum_j D(-t_j - t_{jk}) \circ n_j(-t) \quad (70)$$

z is the signal to noise ratio for this signal during the first receive period. If z is large compared to unity the target information is already in the memory after the first receive period and can be displayed, for example, by cross-correlating the content of one memory element (say $k=0$) with all others and displaying the correlator output. The correlator output $c_k(t)$ for the k th channel follows from eqs. (57), (62) and (64) as:

$$c_k(t) \sim \sum_j a\{t - (t_{jk} - t_j)\} \quad (71)$$

where $a(t)$ is the autocorrelation function of the filter impulse response. The function $a(t)$ takes the place of the search pulse envelope and the display is equivalent to that discussed above in the noise-free case. If z is small compared to unity but g_j large compared to 1, one obtains an improved signal to noise ratio at higher iterations. Using eqs. (65) and (19-24) we find for 2f_k

$$^2f_k = \sqrt{\frac{P}{K}} \sum_j D(-t_j - t_{jk}) (g_j \circ n_j + ^1n_j) g_j + \sqrt{P} D(-^1t^{\beta}) ^1n_k(-t) \quad (72)$$

We see that the signal portion is changed through the incoherent addition of $^1n_j(t)/g_j$ to $\circ n_j(t)$. The new signal to noise ratio z is now

$$^2z = g_j^4 (1 + 1/g_j^2) / K \quad (73)$$

which is improved by the factor of g_j^2 compared to the previous iteration. It is obvious from the foregoing that every additional iteration contributes a factor g_j^2 to the signal to noise ratio.

$$n_z = g_j^{2n} \frac{n}{\sum_{v=1}^n} g_j^{-2(v-1)} / (K \frac{n-1}{\sum_{v=1}^{n-1}} g_j^{-2(v-1)}) \approx (g_j^{2n})/K \quad (74)$$

Equation (74) seems to imply that only the round-trip gain g_j of the system determines the detectability of a target independent of the amount of the additive noise in the receive circuitry. This, however, is not true since the total amplifications factor γ which appears in the expression for g_j is limited in any realizable system by the noise power P_n . If we assume, for example, a maximum rms voltage V_{\max} at the array transducers during transmission and an input impedance of R_i at the preamplifier the maximum total amplification factor γ is

$$\gamma \leq V_{\max} / \sqrt{R_i P_n} \quad (75)$$

For a thermal noise limited system with $P_n = kTB$, for example, one obtains

$$\gamma \leq V_{\max} / \sqrt{R_i kTB} = 1.5 \cdot 10^{10} \frac{V_{\max}}{\sqrt{R_i B}} \quad (76)$$

B is the bandwidth of the system. Equation (76) gives, for example, for $V_{\max} = 10$ KV, $R = 100 \Omega$ and $B = 10$ KHz a limit for the voltage amplification factor of $1.5 \cdot 10^{11}$. If we introduce the maximum value of γ into the equation (39a) for g_j we see that the maximum realizable round-trip gain now depends on the noise power of the system:

$$g_j \leq \frac{\alpha \beta \kappa \sigma_j}{r_j^2} \cdot \frac{V_{\max}}{(R_1 P_n)^{1/2}},$$

where α and β are transducer constants defined in eqs. (9) and (20). If g_j approaches unity, no improvement in signal to noise is obtained by higher iterations.

We shall now briefly consider the case of a search pulse together with additive noise in the system. The search pulse appears for the first time as a third term in the function ${}^1f_k(t)$ equation (64). In order to have the array response dominated by the search pulse rather than the quasi random noise function ${}^1s_k(t)$ we require that the pulse power P_s is very large compared to the noise power P_n and that the round-trip gain g_j is large compared to unity. We then obtain a signal to noise ratio for one target:

$$z \approx \frac{P_s g_j^2}{P_n}$$

which is the equivalent of the case for the quasi random search function ${}^1s_k(t)$ given in equation (69) above.

VI. Reverberation Noise

In this section the effect of volume backscatter (reverberation) on the system performance is considered. Since the system is linear, one can consider again as in the white noise case the response of the system to the noise only. It will be found that the

reverberation received in the first receive period is for a wide class of systems practically uncorrelated between different array elements (channels) so that appreciable array gain can be achieved for the first retransmit cycle. For higher iterations, however, the resulting reverberation noise is highly correlated between channels and no further array gain in signal to noise ratio is possible with higher iterations.

The reverberation environment

The following analysis is based on a statistically uniform distribution of scatterers throughout the search volume. The probability to find one scatterer in a given volume element is proportional to this volume element and proportional to the density ρ of the scatterers. One has therefore:

$$\text{Probability (one scatterer in } dV) = \rho \cdot dV \quad (77)$$

Each scatterer is characterized by a scatterstrength S_j and a velocity v_j . The scatterstrength S_j is a complex random variable of zero mean with the real and imaginary parts jointly gaussian:

$$\begin{aligned} E\{S_j\} &= 0 \\ E\{S_j S_{j'}\} &= \sigma \delta_{jj'} \end{aligned} \quad (78)$$

v_j is the relative velocity of the j th scatterer relative to the array, that is, the velocity component which determines the doppler shift of the back-scattered signal. v_j is again a random variable of zero mean which is also assumed to be gaussian:

$$\begin{aligned} E\{v_j\} &= 0 \\ E\{v_j v_{j'}\} &= \delta_{jj'} \end{aligned} \quad (79)$$

$\delta_{jj'}$ is the Kronecker δ and $E\{x\}$ is the expectation of the random variable x .

The reverberation noise

We consider first the signal received during the first receive period $t^\alpha < t < t^\beta$ caused by the backscatter of the search pulse due to the distribution of point scatterers introduced above. One can treat the scatterers in the same manner as the targets were treated in Section II eq. (19). One obtains for the pressure distribution p_k at the k th element:

$$n_k(t) \approx p_k(t) = \sum_j \frac{S_j}{r_j^2} \exp\{-i\omega_0\{t_j + (t_{jk} + (t_{jk} - t)(1 + v_j/c))\} \bar{f}(t - t_{jk} - t_j)\} \quad (80)$$

In eq. (80) the search pulse $f(t)$ has been written as:

$$f(t) = e^{i\omega_0 t} \bar{f}(t) \quad (81)$$

where $\bar{f}(t)$ is the pulse envelope and ω_0 the center frequency of the search pulse. The factor $(1 + v_j/c)$ in the exponent represents the doppler shift of the backscattered signal. The doppler shift is significant only in the fast varying exponential but negligible in the envelope function.

The noise covariance

The effect of the reverberation noise $n_k(t)$ eq. (80) on the system performance is governed by the covariance function $R_{kk'}(t, \tau)$:

$$R_{kk'}(t, \tau) = E\{n_k^*(t) n_{k'}(t + \tau)\} / E\{|n_k(t)|^2\} \quad (82)$$

The expectation $E\{n_k(t) n_k^*(t + \tau)\}$ is:

$$\begin{aligned} E\{n_k(t) n_k^*(t + \tau)\} = \\ E\left\{ \sum_j \frac{\sigma}{r_j} \exp\{i\omega_0(t_{jk} - t_{jk'} + \tau)\} E\left\{ \exp\{i\omega_0 \frac{v_j}{c}(t_{jk} - t_{jk'} + \tau)\} \right\} \right. \\ \left. \cdot \bar{f}(t - t_{jk} - t_j) \cdot \bar{f}^*(t - t_{jk'} - t_j + \tau) \right\} \end{aligned} \quad (83)$$

The double sum which results if one uses eq. (80) to form the product $n_k(t) n_{k'}(t + \tau)$ reduces by virtue of eq. (78) to the single sum given in eq. (83). Since v_j is gaussian the expectation of the doppler factor under the sum in eq. (83) becomes:

$$\begin{aligned} E\left\{ \exp\{i\omega_0 \frac{v_j}{c}(t_{jk} - t_{jk'} + \tau)\} \right\} = \\ \exp\{-[\omega_0(v/c)(t_{jk} - t_{jk'} + \tau)]^2/8\} \end{aligned} \quad (84)$$

In order to make the evaluation of the expectation of the sum over all scatter contributions tractable, we consider only the case of a line array of equidistant elements and introduce a spherical coordinate system r, ϕ, θ which has its origin at the reference element $k = 0$ of the array, and its polar axis along the array axis. The polar angle θ is defined such that $\theta = 0$ represents the equatorial plane of the coordinate system.

The time delay parameters t_{jk} in eq. (83) depend on the relative position of the j th scatterer and the k th array element:

$$t_{jk} = |\vec{r}_j - \vec{r}_k|/c \quad (85)$$

where \vec{r}_j and \vec{r}_k are the position vectors of the j th scatterer and the k th array element. In our coordinate system $|\vec{r}_j - \vec{r}_k|$ becomes in first order in (d/r_j)

$$|\vec{r}_j - \vec{r}_k| = r_j - d k \sin \theta \quad (86)$$

where d is the distance between array elements.

Introducing eqs. (84) and (86) into eq. (83) one obtains for the sum in eq. (83):

$$\sigma \sum_j \frac{1}{r_j} \exp\{i\omega_0(s+\tau) - [(s+\tau)\omega_0 v/c]^2/8\} \circ f(u_j + \frac{ks}{k'-k}) \circ f^*(u_j + \frac{k's}{k'-k} + \tau) \quad (87)$$

where

$$s = (k' - k)d \sin \theta / c$$

$$u_j = t - \frac{2r_j}{c} \quad (88)$$

To evaluate the expectation of the sum over all scatter contributions eq. (87), one replaces the sum over all scatterers by the sum over all volume elements which make up the acceptance cone of the system and multiplies each term of the sum with the probability of finding a scatterer in the corresponding volume element. One can always make the volume elements so small that the probability becomes negligible to find more than one scatterer in the

volume element. The occurrence of a scatterer in a volume element is then a random variable which has as its range only the values zero and one. The probability that the value is one is according to eq. (77) equal to ρdV . The expectation of the sum, therefore, is equal to the integral

$$E\{\Sigma_j\} = \frac{16\rho\sigma}{c^4} \int_{\text{Search Volume}} (t-u)^{-4} \exp\{i\omega_0(s+\tau) - [\omega_0(s+\tau)\frac{v}{c}]^2/8\} \quad (89)$$

$$\cdot \circ \bar{f}(u + \frac{sk}{k' - k}) \circ \bar{f}^*(u + \frac{sk'}{k' - k} + \tau) dV$$

The coordinate of the j th scatterer r_j has been replaced by the coordinate r of the corresponding volume element. The new variable u replaces u_j of eq. (88)

$$u = t - \frac{2r}{c} \quad (90)$$

and the volume element dV is given by:

$$dV = r^2 dr \cos\theta d\theta d\phi = \frac{c^4}{8(k' - k)d} (t-u)^2 du ds d\phi \quad (91)$$

The integral is taken over the acceptance cone of the system.

The acceptance cone is defined by the radiation pattern of the individual array elements and by the range R from which echoes are accepted during the first receive period.

It is sufficient for the purpose of the present analysis to identify the acceptance cone with the main lobe of the radiation pattern of a quadratic array element of side a :

$$\begin{aligned}\phi &\leq \phi_{\max} = \arctg \frac{\lambda}{2a} \\ \theta &\leq \theta_{\max} = \arctg \frac{\lambda}{2a}\end{aligned}\quad \text{for } a \geq \lambda/2 \quad (92)$$

The acceptance range is

$$R_{\min} - A - \tau_0 c \leq r \leq R_{\max} + A + \tau_0 c \quad (93)$$

where $A = Kd$ is the array aperture.

The integral eq. (89) can be simplified by neglecting the doppler term $\exp\{-[\omega_0(s+\tau)v/c]^2/8\}$. According to eq. (88) the term $\omega_0(s+\tau)v/c$ is limited by

$$\omega_0(s+\tau)v/c < 2\pi\left(\frac{A}{\lambda} + \tau v\right)v/c \quad (94)$$

Since v/c is of the order of 10^{-5} , one can neglect the doppler shift even for very large arrays and long search pulses. Introducing the volume element eq. (91) into eq. (89) and integrating over ϕ , one obtains:

$$E\{\Sigma j\} = \frac{4\phi_m^{\sigma \cdot \rho}}{(k'-k)dt^2} \int_{u_{\min}}^{u_{\max}} \int_{-|s|_{\max}}^{|s|_{\max}} \frac{e^{i\omega_0(s+\tau)}}{(1 + \frac{u}{t})^2} \quad (95)$$

$$\cdot \bar{f}\left(u + \frac{sk}{(k'-k)}\right) \bar{f}^*\left(u + \frac{sk'}{k'-k} + \tau\right) du ds$$

where u_{\max} and u_{\min} and $|s_{\max}|$ are given by

$$u_{\max} = \frac{t}{2} - \frac{R_{\min}}{c} + \frac{A}{c} + \tau_0 \quad (96)$$

$$u_{\min} = t/2 - \frac{R_{\max}}{c} - A/c - \tau_0$$

$$|s_{\max}| = \frac{|(k'-k)|d \sin \theta_{\max}}{c} \approx |k'-k| \frac{d\lambda}{2ac} = |k'-k|vd/2a$$

We shall now show that one can extend the integration over u from $-\infty$ to $+\infty$ without changing the value of the integral in eq. (95).

The time interval of interest is the first receive period $t^\alpha < t < t^\beta$. It is given by:

$$\frac{R_{\min}}{c} - \frac{A}{2c} < \frac{t}{2} < \frac{R_{\max}}{c} + \frac{A}{2c} + \tau_0 \quad (97)$$

It follows from eqs. (96) and (97) that during the first receive period u_{\min} is always smaller than $-A/2c$ and u_{\max} always larger than $A/2c + \tau_0$. The pulse envelope $f(u + \frac{sk}{k^1 - k})$, however, and, therefore, the integrand in eq. (95) is unequal to zero only for

$$0 \leq u + \frac{sk}{k^1 - k} \leq \tau_0 \quad (98)$$

Since by definition $|\frac{sk}{k^1 - k}|$ is smaller than $A/2c$, one obtains as the condition for a non-vanishing integrand

$$-A/2 < u < A/2 + \tau_0 \quad (99)$$

It follows, therefore, that the domain of integration over u : $u_{\min} < u < u_{\max}$ always includes the region where the integrand is unequal zero for any choice of t within the first receive period. The integral is, therefore, independent of t and does not change its value if the boundaries are extended to $\pm \infty$.

We observe further that the lower bound for t (eq. 97) is $R_{\min} - \frac{A}{2}$, and that the upper bound of u for which the integrand is not equal to zero is:

$$u = \frac{A}{2c} + \tau_0 \quad (100)$$

one obtains, therefore, an upper bound for u/t by:

$$u/t < \frac{A + 2\tau_0 c}{2R_{\min}} + 0\left(\frac{A}{R_{\min}}\right)^2 \quad (101)$$

Since both A and $\tau_0 c$ are small compared to R_{\min} for all practical systems, we can in good approximation neglect the term $(1 + \frac{u}{t})^2$ in the integral of eq. (95) and obtain:

$$E\{\Sigma\}_j = \frac{Ct^{-2}}{(k'-k)} \int_{-\infty}^{+\infty} \int_{-|s_{\max}|}^{+|s_{\max}|} \exp\{i\omega_0(s+\tau)\} \quad (102)$$

$$\cdot {}^\circ \bar{f}\left(u + \frac{sk}{k'-k}\right) {}^\circ \bar{f}^*\left(u + \frac{sk}{k'-k} + s+\tau\right) du ds$$

where $C = \frac{4\phi_m \sigma \rho}{a}$. The argument of ${}^\circ \bar{f}^*$ was obtained by observing that $\frac{k's}{k'-k} = \frac{ks}{k'-k} + s$. We introduce the new variables

$$v = u + \frac{sk}{k'-k} \text{ and } x = s + \tau \quad (103)$$

and obtain

$$E\{\Sigma\}_j = \frac{C \int_{-\infty}^{+\infty} |\bar{f}|^2 dv}{(k'-k)t^2} \int_{-|s_{\max}|}^{+|s_{\max}|} A(x) e^{i\omega_0 x} dx \quad (104)$$

where $A(x)$ is the normalized autocorrelation function of the pulse envelope:

$$A(x) = \frac{\int_{-\infty}^{+\infty} {}^\circ \bar{f}(v) {}^\circ \bar{f}^*(v+x) dv}{\int_{-\infty}^{+\infty} |{}^\circ \bar{f}(v)|^2 dv} \quad (105)$$

To evaluate $R_{kk}, \{t, (t+\tau)\}$ as defined in eq. (82), we have to determine the function $E\{\Sigma\}_j$ for $t = {}^\circ t_\alpha$, $\tau = 0$ and $k = k'$:

$$E\{|n_k({}^\circ t^\alpha)|^2\}_j = E\{\Sigma\}_j \Big|_{\substack{t=t_\alpha \\ \tau=0 \\ k'=k}} = C ({}^\circ t^\alpha)^{-2} \int_{-\infty}^{+\infty} |\bar{f}|^2 dv \lim_{k \rightarrow k'} \frac{2|s_{\max}|}{(k'-k)} \quad (106)$$

$$= C ({}^\circ t^\alpha)^{-2} \int_{-\infty}^{+\infty} |\bar{f}|^2 dv \cdot \frac{d}{a} v$$

Combining eqs. (104) and (106) we finally obtain for the covariance function $R_{kk}, (t, t+\tau)$:

$$R_{kk}(t, t+\tau) = \frac{(\sigma t_\alpha)^2}{2(s_{\max})^2} \int_{-|s_{\max}|}^{|s_{\max}|} A(x) e^{i\omega_0 x} dx \quad (107)$$

It is sufficient for the following to suppress the time dependence in $R_{kk}(t, (t+\tau))$ and consider only its maximum $R_{kk}(\sigma t_\alpha, \tau)$ which we denote as $R_{kk}(\tau)$. The integral in eq. (107) which is independent of t can be formally integrated. To do so we rewrite eq. (96) as:

$$R_{kk}(\tau) = \frac{1}{|s_{\max}|} \int_{-\infty}^{+\infty} \text{rect}_{|s_{\max}|}(x-\tau) \text{rect}_{\tau_0}(x) A(x) e^{i\omega_0 x} dx \quad (108)$$

The rectangular function $\text{rect}_y(x)$ is defined as

$$\text{rect}_y(x) = \begin{cases} 1 & \text{for } |x| < y \\ 0 & \text{otherwise} \end{cases} \quad (109)$$

The first function $\text{rect}_{s_{\max}}(x-\tau)$ in eq. (107) was introduced to change the limits of the integral; the second rectangular function $\text{rect}_{\tau_0}(x)$ was introduced to set in evidence the fact that the autocorrelation function $F(x)$ of the pulse envelope is zero for $|x|$ greater than the search pulse duration

$$A(x) = \text{rect}_{\tau_0}(x) A(x) \quad (110)$$

To integrate eq. (108) we consider two cases:

$$\text{a.) } |s_{\max}| > \tau_0 \quad \text{and} \quad \text{b.) } |s_{\max}| < \tau_0$$

The first case corresponds to widely spaced elements. We shall show that in this case the correlation function $R_{kk}(\tau)$ is very small.

To simplify the integral eq. (108) we consider that the product of two rectangular functions can always be reduced to a single rectangular function.

We have:

$$\begin{aligned} & \text{rect}_{\tau_0}(x) \\ & \text{for } |\tau| \leq |s_{\max}| \leq \tau_0 \\ \text{rect}_{s_{\max}}(x-\tau) \text{rect}_{\tau_0}(x) = & \text{rect}_{\alpha}(x-\beta) \quad (111) \\ & \text{for } |s_{\max}| - \tau_0 < \tau < |s_{\max}| + \tau_0 \\ & 0 \quad \text{for } |\tau| > |s_{\max}| + \tau_0 \end{aligned}$$

with

$$\alpha = \{|s_{\max}| + \tau_0 - |\tau|\}/2$$

$$\beta = \{\tau_0 - |s_{\max}| + |\tau|\}/2$$

We need to consider only the first case which includes the important domain around $\tau = 0$. Because of eqs. (110) and (112) the integral eq. (108) reduces to the power spectrum $F(\omega)$ of the pulse envelope:

$$R_{kk'}(\tau) = \frac{1}{2s_{\max}} F(\omega_0) \text{ for } |\tau| < |s_{\max}| - \tau_0 \quad (112)$$

with

$$F(\omega_0) = \int_{-\infty}^{+\infty} A(x) e^{i\omega_0 x} dx$$

Note that $R_{kk'}(\tau)$ does not depend on τ as long as $|\tau|$ is smaller than $|s_{\max}| - \tau_0$.

The power spectrum of the pulse envelope at the carrier frequency $\omega = \omega_0$ is very small even for short pulses. We consider as an example a pulse with a gaussian envelope and a time constant $\tau_0 = 3/v$. Its power spectrum $F(\omega_0)$ becomes:

$$F(\omega_0) = \frac{3\sqrt{\pi}}{2v} e^{-\frac{(3\pi)^2}{2}} \quad (113)$$

which is zero for all practical purposes.

We consider now the second case which corresponds to closely-spaced elements. Here once again correlation between elements is relatively small.

The product of the two rectangular functions in the integral eq. (109) reduces in this case to the rectangular function:

$$\begin{aligned} \text{rect}_{s_{\max}}(x-\tau) \text{rect}_{\tau_0}(x) &= \begin{aligned} &\text{rect}_{s_{\max}}(x-\tau) \\ &\text{for } |\tau| < \tau_0 < |s_{\max}| \\ &\text{rect}_{\alpha}(x-\beta) \\ &\text{for } \tau_0 - |s_{\max}| < \tau < \tau_0 + |s_{\max}| \\ &0 \quad \text{for } \tau > \tau_0 + |s_{\max}| \end{aligned} \end{aligned} \quad (114)$$

with

$$\alpha = \{|s_{\max}| + \tau_0 - |\tau|\}/2$$

$$\beta = \{\tau_0 + |\tau| - s_{\max}\}/2$$

We consider again the first domain of τ in eq. (114)

and find from eq. (109):

$$R_{kk'}(\tau) = e^{i\omega_0\tau} \{\text{sinc}(s_{\max}\omega) * F(\omega)\}_{\omega=\omega_0} \text{ for } |\tau| < \tau_0 - |s_m| \quad (115)$$

The convolution of the sinc function with the narrower pulse-like power spectrum $F(\omega)$ leaves the sinc function virtually unchanged so that we have in good approximations for small values of τ :

$$R_{kk'}(\tau) \approx \text{sinc}(\omega_0 s_{\max}) = \text{sinc}\left(\frac{\pi(k-k')d}{a}\right) \quad (116)$$

For a dense array with $d = a/2$ the correlation of the noise between neighboring channels is zero in our approximations and is not very high for non-integral d/a , which is by definition larger than unity.

Any coupling, however, is undesirable since the re-emitted reverberation noise from correlated channels adds coherently at targets of interest and one can, therefore, not get the full array gain in signal to noise ratio during the following iteration. One can, however, reduce the correlation even farther by increasing the element spacing. A more effective decoupling of the noise in neighboring channels is obtained by increasing both the array spacing and the search pulse bandwidth so that even for adjacent channels the condition $|s_{\max}| > \tau_0$ discussed under a.) holds. This requires an element spacing:

$$d > a(\tau_0 v) = n \cdot a \quad (117)$$

where n is the number of oscillations in the pulse and a the element diameter. With such an element spacing the reverberation noise in all channels is virtually uncorrelated and we can treat the noise as far as its interaction with desired targets is concerned in the same manner as we treated the white noise in Section 3.

We have to consider, however, also the interaction of the retransmitted noise with the field of undesired scatterers. If the scatterers were stationary, the time inverted retransmitted noise signal would generate as we have seen in Section 1 a strong pulse-like backscattered signal proportional to the autocorrelation function of the scatter distributions. The motion of the scatterers, however,

during the time interval between transmissions reduces this correlation by a factor

$$e^{-\left\{\frac{2\pi v v}{c}(\alpha t - t_{\beta})\right\}^2} \approx e^{-\left(\frac{8\pi v R_{\max}}{c\lambda}\right)} \quad (118)$$

This factor had been given in eq. (84). It is in the present case zero for all practical purposes. One can, therefore, proceed with the first iteration in the same manner as was done in the white noise case discussed above. With the result, that one obtains almost the full array gain of K in signal to noise ratio. The difference between the reverberation noise and the white noise case becomes apparent at the second system cycle which begins with the second retransmission. If targets are present, the system now transmits essentially insonification beams focused on the targets. To simplify the issue we assume the presence of only one target, therefore, of one transmitted beam. The reverberation noise due to the retransmitted beam (if we neglect the side lobe contribution which was justified in Section 2) is very similar to that calculated above with the important exception that the acceptance cone is now determined by the aperture of the array A and not the aperture of a single element a . θ_{\max} , therefore, becomes now

$$\theta_{\max} = \arctg \frac{\lambda}{A} = \frac{\lambda}{Kd} \quad (119)$$

and therefore

$$|s_{\max}| = \frac{(k-k')d\theta_{\max}}{c} = \frac{(k'-k)}{K \cdot v} = \frac{k'-k}{Kv} \quad (120)$$

Equation (123) shows that $|s_m|$ is even for the most distant elements much smaller than τ_0 .

We obtain, therefore, in analogy to eq. (119) for the covariance function of the reverberation noise generated in the second system cycle

$$l_{R_{kk'}}(\tau) \approx \text{sinc}\left(\frac{\pi(k-k')}{K}\right)$$

Since $|k-k'|$ is smaller than $K/2$ the noise in all channels is highly correlated and further iteration does not increase the signal to noise ratio.

This behavior of the system is demonstrated in the next section by computer model studies.

VII. Computer Simulation of System Operations in Reverberating Environment

A computer model was constructed to study the behavior of the time inversion system in a reverberation environment. In this section the model is described, the program listing given and results of the study presented.

The Model

The model calculations are based on a linear receive transmit array which operates against a two dimensional target field. A cartesian coordinate system x,y is used to describe the relative positions of array and targets. The array is located on the y axis of the coordinate system. It consists of $K = 2^n$

equally spaced elements. The distance d between elements is equal to the wavelength λ of the carrier frequency ν . The unit of time is the period $T = \frac{1}{\nu}$ of the carrier frequency and the unit of length the wavelength λ . This convention reduces the frequency ν , the wavelength λ and the signal velocity c to unity. The array elements are numbered from $-(\frac{K}{2} - 1) < k < K/2$ with the element $k = 0$ coinciding with the origin of the coordinate system. The target field consists of a single point Target of Strength S surrounded by a random distribution of scatterers. The target is located on the x -axis at $x = R_0$. The scatterers are distributed over the rectangular area $R_0/2 \leq x \leq \frac{3}{2} R_0$; $-R_0 \leq y \leq +R_0$, which is centered at the target.

The total number of scatterers is N . The position vectors $r_j = \{x_j ; y_j\}$, $j = 1, 2, \dots, N$ of the scatterers are generated by the computer as part of the simulation program.

The scatter strength σ_j of the scatterers which appears always together with the range r_j of the scatterer as (σ_j/r_j^2) is replaced in the following by its mean $\langle \sigma_j/r_j^2 \rangle$ and normalized to $1/R_0^2$. The normalization is possible since the significant parameter in the simulation is the relative scatter strength S of the actual target.

The Simulation of the System Operations

The target acquisition process begins as in all previous examples with the emission of a gaussian search pulse, which is because of the conventions adopted above:

$$\phi(t) = \exp\{i2\pi t - t^2/\tau\}$$

This pulse is scattered back by all scatterers in the field and by the target proper. Taking into account the normalization of the individual scatter cross sections, one obtains for the first backscattered signal:

$$x_k^1(t) \sim \left\{ \sum_{j=1}^N \delta(t-t_j-t_{jk}) + S \cdot \delta(t-t_0-t_0k) \right\} * \phi(t) \quad (121)$$

with

$$t_{jk} = r_{jk} = (x_j^2 + (y_k - k)^2)^{1/2}$$

$$t_j = t_{j0} \text{ and } t_0 = R_0$$

The function $x_k^1(t)$ has to be sampled at intervals $\Delta t = \frac{1}{2B}$ where B is the bandwidth of the search pulse:

$$B = \frac{2}{\tau} \quad (122)$$

The sampling interval is therefore:

$$\Delta t = \tau/4 \quad (123)$$

The time interval over which $x_k(t)$ is to be observed is the first receive period: $\phi t^\beta - \phi t^\alpha$. In our model because of the convention $c = 1$ we have:

$$\phi t^\beta - \phi t^\alpha = 2(R_{\max} - R_{\min}) + \tau + K = \approx 4R_0 \quad (124)$$

The required minimum number of samples M to describe the function $x_k^1(t)$ is therefore:

$$M = \frac{\phi t^\beta - \phi t^\alpha}{\Delta t} = \frac{16 R_0}{\tau} \quad (125)$$

It is more efficient to perform the actual calculation in the Fourier domain. The Fourier transform $\tilde{X}_k^1(v)$ of $X_k^1(t)$ is given by:

$$\tilde{X}_k^1(v) \approx \left\{ \sum_{j=1}^N e^{-i2\pi v(r_j + r_{jk})} + S e^{-i2\pi v(r_o + r_{ok})} \right\} \cdot e^{-\frac{(\pi(v-1)\tau)^2}{2}} \quad (126)$$

The sampling intervals Δv are given by:

$$\Delta v = \frac{1}{2(\tau^\beta - \tau^\alpha)} = \frac{1}{8R_o} \quad (127)$$

and since M samples have to be taken, v ranges between

$$1 - M/2 \Delta v < v < 1 + M/2 \Delta v \quad (128)$$

or: $1 - \frac{1}{\tau} < v < 1 + \frac{1}{\tau}$

The frequency band is centered around the carrier frequency which according to the adopted convention is equal to 1.

The calculation of X_k^1 implies the calculations of $K \times M$ sums over the echoes from the N scatterers. The actual results shown later are based on 1000 randomly distributed scatterers.

In order to reduce the amount of calculation, we replace r_{jk} by a linear approximation

$$r_{jk} = \sqrt{x_j^2 + (y_j^2 - k)^2} = r_j - \frac{y_j k}{r_j} \quad (129)$$

and replace the sum over j in eq. (126) which has in our model 1000 terms by a sum over 100 equally spaced phase terms in the following manner:

$$\sum_{j=1}^N e^{i2\pi\{v(2r_j + k \frac{y_j}{r_j})\}} = \sum_{\ell=1}^{100} a(v, k)_\ell \cdot e^{i2\pi \frac{(\ell-.5)}{100}} \quad (130)$$

where $a(v, k)_\ell$ is the number of occurrences that the fractional part of $v \cdot (2r_j + k \frac{y_j}{r_j})$ falls between $\frac{\ell-1}{100}$ and $\ell/100$. The $x_k^1(v)$ calculated in our program is therefore:

$$x_k^1(v) = \left\{ \sum_{\ell=1}^{100} a(v, k)_\ell e^{i2\pi(\ell-.5)/100} + S e^{i2\pi v R_0} \right\} \cdot e^{-\{(v-1) \cdot \pi \tau\}^2} \quad (131)$$

The computation of $x_k^1(v)$ is executed in two steps. The first step evaluates $x_k^1(v)$ with no target present that is for $S = 0$. The result is then put on tape (identified as tape 16 in the program). The second step is to combine this with a target response. This partition has been made to facilitate experimenting with different target sizes, locations and numbers.

The program listings are given in Tables 1 and 2. The inputs to the program are the pulse duration τ identified as TW, the target position R_0 , the number of array elements K , the target strength S and the total number of scatterers N .

The Second and Higher Iterations

The second iteration $x_k^2(t)$ represents the return from the retransmitted time inverted signal $x_k^1(t)$ and is given by:

$$x_k^2(t) \sim \sum_{k'} \left\{ \sum_j \delta(t - t_{jk}, -t_{jk} + \gamma_j) + S/\delta(t - t_{ok} - t_{ok'}) \right\} \cdot x_{k'}^{(1)}(-t) \quad (132)$$

The term γ_j in the time delay operator of eq. (127) represents an approximation to the effect of the motion of the scatterers. γ_j is a random number which represents the displacement of the scatterer which occurred between successive pings. γ_j is gaussian with a variance of 2π generated in the program. Introducing the same approximations and conventions as in evaluating $x_k^{(1)}$ we obtain for the Fourier transform of $x_k^2(v)$:

$$x_k^2(-v) \approx \sum_{k'} \left\{ \sum_j e^{-i2\pi v(2r_j^2 + \gamma_j(k-k')/r_j + \gamma_j)} + S e^{-i4\pi v r_0} \right\} \cdot x_{k'}^1(v) \quad (133)$$

Here again we approximate the sum over j by:

$$\sum_j e^{-2\pi\{v(2r_j + \gamma_j(k-k')/r + \gamma_j)\}} = \sum(\nu\kappa) = \sum_{\kappa=1}^{100} a(\nu\kappa) e^{-2\pi(\kappa-.5)/100}$$

where $\kappa = (k-k')$. κ can assume 2 K different values for which $\sum(\nu\kappa)$ is evaluated. $x_v^2(-v)$ then becomes:

$$x_k^2(v) = \sum_{\kappa=k-\frac{K}{2}}^{k+K/2} (\sum(\nu\kappa) + S e^{-2\pi\nu R_0}) x_{k-\kappa}^1(v)$$

The calculation of $x_k^2(-v)$ is again executed in two steps - first for $S = 0$:

$$\{x_k^2(-v)\}_{S=0} = \sum_{\kappa=k-\frac{K}{2}}^{k+K/2} \sum(\nu\kappa) x_{k-\kappa}^1(v)$$

and then for the return with target

$$X_k^2(-v) = \{X_k^2(-v)\}_{S=0} + \sum_{\kappa=k-K/2}^{k+K/2} S e^{-4\pi v R_0} \cdot X_{k-\kappa}^1(v)$$

The program listings are given in Tables 3 and 4. The Fourier transform of the first and second and high iteration returns $X_k^1(v)$ and $X_k^2(v)$ were transformed back into the time domain by the Fourier transform and plotting routine given in Table 5.

To compute the third iteration the return-functions $X_k^2(v)$, which is given by the program in the frequency domain, has to be transformed back into the time domain $X_k^2(t)$ and multiplied with a window function to account for the narrow odd receive periods (see Fig. 1). This truncated set of functions $\overline{X_k^2}t$ is then transformed back into the frequency-domains to give $\overline{X_k^2}(v)$.

The third iteration then follows in complete analogy to the second one by

$$X_k^3(v) = \sum_{\kappa=k-K/2}^{k+K/2} \{ \Sigma(-v, \kappa) + S \cdot e^{-4\pi v R_0} \} X_k^2(v)$$

Results of the Simulations

The program described above is capable of handling multiple targets and a wide range of search pulse bandwidths.

Due to budgetary constraints, it was only possible to consider a small system of 32 elements operating against a single target with a narrow band search pulse.

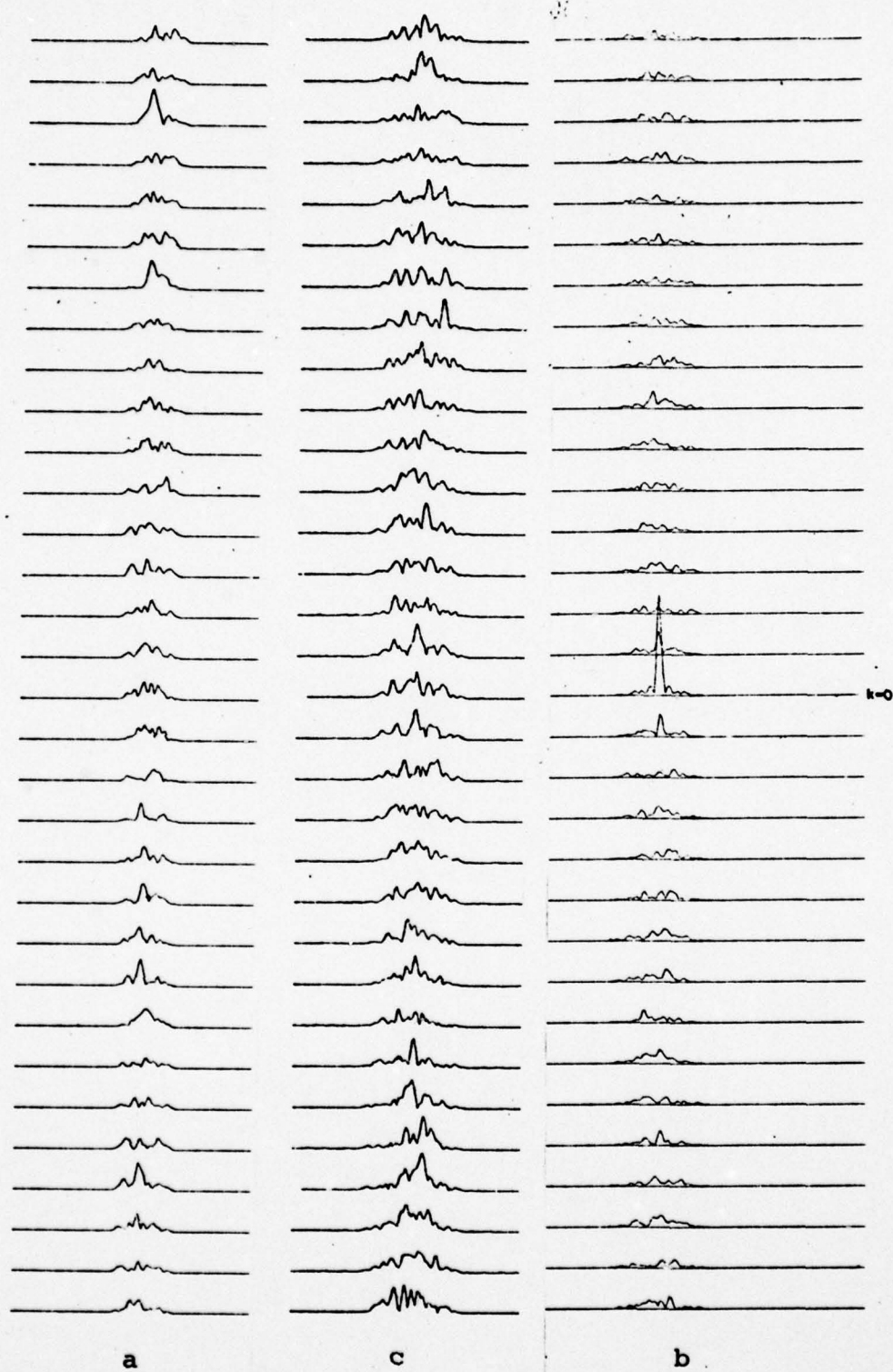


Fig. 6

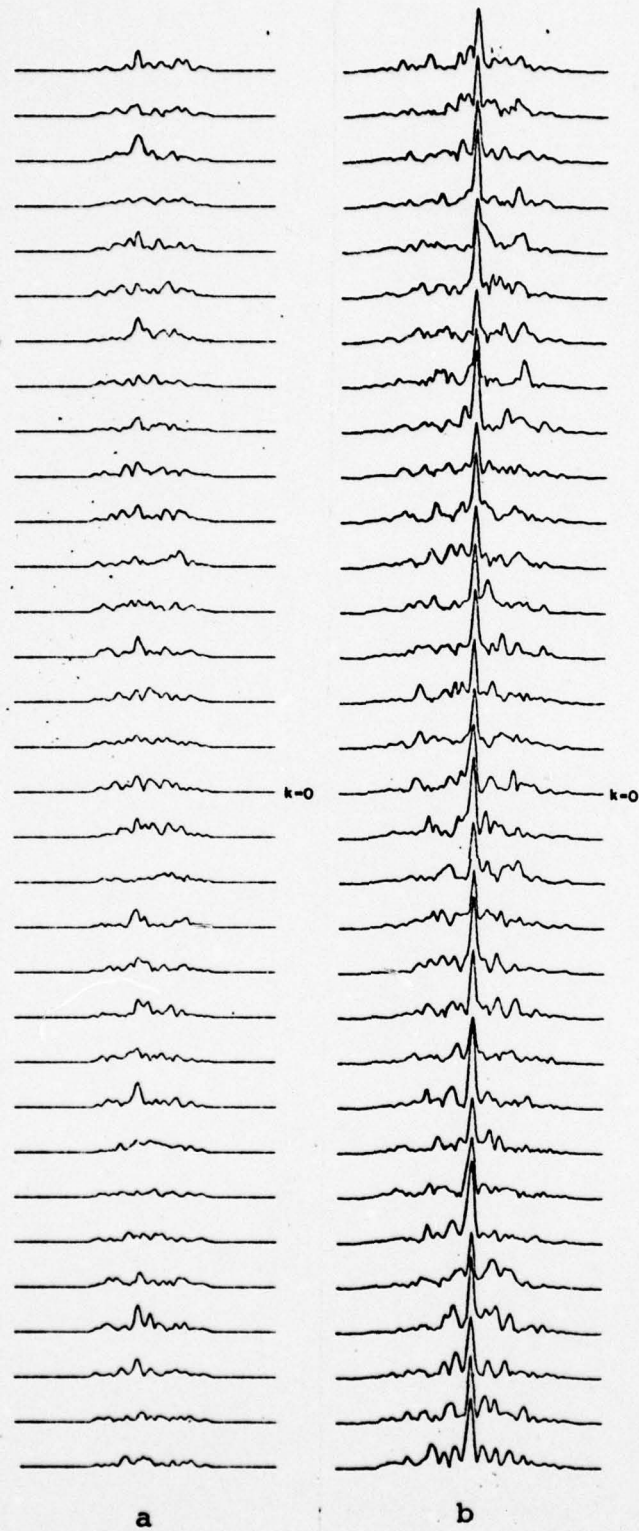


Fig. 7

A target range of $R_0 = 1000$ and a pulse width of $\tau = 160$ was chosen. This made it possible to handle the return with 128 frequency or time samples.

In Fig. 6a the return signal $x_k^1(t)$ without a target in the field is shown for all 32 channels.

In Fig. 6b the first iteration return $x_k^2(t)$ is shown for the case that all scatterers are stationary. The return signal to the reference element is essentially the autocorrelation of the reverberation noise. The signal in the channels $k \neq 0$ gives a measure of the noise correlations in separate channels. It can be seen that the correlation is still substantial in the nearest neighbor channels but has practically disappeared in all other channels.

In Fig. 6c the first iteration return is shown with the scatterer motions taken into account. The second return $x_k^2(t)$ is now essentially noise-like similar to $x_k^1(t)$ as is to be expected.

In Fig. 7a the return signal $x_k^1(t)$ is shown with a target of strength $S = 15$ present in the field. The signal still looks essentially noise-like. The target cannot be recognized. Figure 7b shows the first iteration $x_k^2(t)$ with the target in place. The target is now clearly visible. This is due to the residual array gain which is smaller than the array gain ($=K$) against uncorrelated noise, but which, due to the low correlation of the noise in channels more than two elements apart (see Fig. 6b), is still appreciable.

VIII. Conclusion

A new concept of a retrodirective self-focussing sonar or radar system has been introduced. The new concept is based on time reversal effected by storing and re-emitting the received signals. The memory requirements for its implementation are discussed and it was shown that state of the art serial access memories are compatible with the system requirements.

The motion sensitivity of the system was analyzed. It was found that the system is compatible with an aggregate of free-floating sonobouys. It was further shown that the motion effect on a system mounted rigidly on a moving platform can be largely compensated by an appropriate shift in the clock-rate which governs the data flow through the memory.

A computer model to simulate the response of the system to reverberation noise has been developed and completed. However, funds were insufficient to use the model for more than the simulation of a very simple low data-rate case.

References

1. L. Van Atta, U.S. Patent 2908002.
2. C. C. Cutler, R. Kompfner, and L. C. Tillotson,
Bell Syst. Tech. J. 42, 2013 (1963).
3. E. L. Gruenberg, H. P. Raabe, and C. T. Tsitsona,
I.B.M. Tech. J. 18, 149 (1974).

Appendix I

Listing of the Program
to Calculate Iterative Returns Without Noise

THIS PAGE IS BEST QUALITY PRACTICABLE
FROM COPY FURNISHED TO DDC

```

1. PROGRAM SONAR(INPUT,OUTPUT,TAPE5=INPUT,TAPE6=OUTPUT)
2. COMMON X(5),SIGMA(5),RIO(5),RIK(5,513),PUJ(5,5)
3. COMMON CUJ(5,5),LUJK(5,5,32),KUJK(5,5,32)
4. COMMON YP(512),YH(512),THAS(2048),FKC(2048)
5. REAL NU,LUJK,KUJK,NU1
6. COMMON/CONFET/TG(1024),NTABLE
7. COMPLEX FKC,IO,SUM,TERM,THAS,SUM2,CONST7
8. PI=3.1416
9. PI2=2*3.1416
10. WRITE(6,9)
11. 3 FORMAT(6X,*TARGET NO.*,5X,*SIGMA*,10X,*X*,11X,*2*)
12. READ(5,11) NTARG
13. 11 FORMAT(I2)
14. DO 1 I=1,NTARG
15. READ(5,12) SIGMA(I),X(I),Z
16. 12 FORMAT(3(F15.8,5X))
17. WRITE(6,13) I,SIGMA(I),X(I),Z
18. 13 FORMAT(7X,4X,I2,7X,E15.6,3X,E15.6,3X,E15.5)
19. XK=-256.
20. DO 2 J=1,513
21. RIK(I,J)=SORT(7*Z+(X(I)-XK)**2)
22. 2 XK=XK+1.
23. RIO(I)=RIK(1,257)
24. 1 CONTINUE
25. READ(5,12) TAU,GAMMA
26. WRITE(6,14) TAU,GAMMA
27. 14 FORMAT(8X,*TAU = *,F15.7,* GAMMA = *,F15.7)
28. DO 5 I=1,NTARG
29. CONST=X(I)/RIO(I)
30. DO 6 J=1,NTARG
31. PUJ(I,J)=CONST-(X(J)/RIO(J))
32. 6 CONTINUE
33. 5 CONTINUE
34. DO 7 I=1,NTARG
35. DO 8 J=1,NTARG
36. CUJ(I,J)=2*(RIO(I)-RIO(J))
37. 8 CONTINUE
38. 7 CONTINUE
39. XMAX=0.
40. DO 10 J=1,NTARG
41. 10 XMAX=XMAX+((SIGMA(J)+GAMMA)/(RIO(J)*RIO(J)))**2
42. XMAX=513.*XMAX
43. XMAX=XMAX+1.3
44. XMAX1=XMAX/10000.
45. TKJMIN=0
46. DO 20 I=1,NTARG
47. IF(X(I).LE.0.) 21,22
48. 21 TKJTEMP=-RIK(I,513)+RIO(I)
49. GO TO 23
50. 22 TKJTEMP=-RIK(I,1)+RIO(I)
51. 23 IF(TKJTEMP.LT.TKJMIN) TKJMIN=TKJTEMP
52. 20 CONTINUE
53. TKJMAX=0.
54. DO 30 I=1,NTARG
55. IF(X(I).GT.0.) 31,32
56. 31 IF(X(I).GT.256.) 33,34
57. 33 ITEMP=513
58. GO TO 35
59. 34 ITEMP=X(I)+257.
60. GO TO 35
61. 32 IF(X(I).LT.-256.) 36,37
62. 36 ITEMP=1
63. GO TO 35
64. 37 ITEMP=X(I)+256.

```

THIS PAGE IS BEST QUALITY PRACTICABLE
FROM COPY FURNISHED TO DDG

```

65. 35 TKJTEMP=-RIK(I,ITEMP)+RIO(I)
66. IF(TKJTEMP.GT.TKJMAX) TKJMAX=TKJTEMP
67. 30 CONTINUE
68. DELTANU=PI/(TKJMAX-TKJMIN+PI2*TAU)
69. TMAX=(TKJMAX-TKJMIN+PI2*TAU)/2.
70. NIT=4*PI/(TAU*DELTANU)
C- CALCULATE LOG BASE 2 OF NUMBER OF DATA POINTS
71. DO 110 NSTAGE=1,20
72. IF(2**NSTAGE.GE.NIT) GO TO 120
73. 110 CONTINUE
74. 120 NIT=2**NSTAGE
75. MUSTRI=-NIT*DELTANU/2.
C- ISTEP IS THE INCREMENT BETWEEN ARRAY ELEMENTS
C- FOR WHICH DATA IS TO BE CALCULATED
C- ISTEP SHOULD BE A POWER OF 2, 1 .LE. ISTEP .LE. 256
76. ISTEP=32
77. NK=512/ISTEP
C- CALCULATE LJK, KJK
78. DO 290 J=1,NTARG
79. DO 280 K=1,NK+1
C- IK IS THE ACTUAL ARRAY ELEMENT WHEN THEY ARE NUMBERED (1,513)
80. IK=(K-1)*ISTEP+1
81. TEMP1=TKJMIN+RIK(J,IK)-RIO(J)
82. TEMP2=TKJMAX+RIK(J,IK)-RIO(J)
83. DO 250 J1=1,NTARG
C- DO NOT USE THIS ON LEADING TERMS
84. IF(J.EQ.J1) GO TO 250
85. KJK(J,J1,K)=(TEMP1+CJJ(J,J1))/ABS(BJJ(J,J1))
86. LJK(J,J1,K)=(TEMP2+CJJ(J,J1))/ABS(BJJ(J,J1))
C- KJK CAN BE NO LESS THAN -256
87. IF(KJK(J,J1,K).LT.-256) KJK(J,J1,K)=-256
C- LJK CAN BE NO MORE THAN 256
88. IF(LJK(J,J1,K).GT.256) LJK(J,J1,K)=256
89. 250 CONTINUE
90. 280 CONTINUE
91. 290 CONTINUE
C CORRECTION FACTOR SQRT(PI)*TAU*DELTANU/(2*PI)
92. PISORT=TAU*DELTANU*.2820948
93. TAUSQ4=(TAU*TAU)/4.
94. NK=NK/2
95. DO 999 K=1,NK+1
C- ZERO OUT FK
96. DO 450 II=1,2048
97. 450 FK(II)=(0.,0.)
98. IK=(K-1)*ISTEP+1
99. NU=MUSTRI
C- IK1 IS ACTUAL ARRAY ELEMENT WHEN NUMBERED (-256,256)
100. IK1=IK-257
C- CALCULATION OF FK(NU)
C
101. DO 490 I=1,NIT
102. SUM=(0.,0.)
103. SUM2=(0.,0.)
104. TERM=(0.,0.)
105. DO 480 J=1,NTARG
106. CONST=PI2+NU
107. CONST1=PISORT*EXP(-NU*NU*TAUSQ4)
108. AJ=(SIGMA(J)*GAMMA)/(RIO(J)*RIO(J))
109. DO 470 J1=1,NTARG
110. IF(J.EQ.J1) GO TO 470
111. AJ1=(SIGMA(J1)*GAMMA)/(RIO(J1)*RIO(J1))
112. BJ=ABS(BJJ(J,J1))
C- IF LJK .LT. KJK HASH TERM IS ZERO

```

THIS PAGE IS BEST QUALITY PRACTICABLE
FROM COPY FURNISHED TO DDC

```

113.      IF (LJJK(J,J1,K).LT.KJJK(J,J1,K)) GO TO 470
114.      CONST3=(CONST+RJ)/2.
115.      CONST4=LJJK(J,J1,K)-KJJK(J,J1,K)+1
116.      CONST5=SIN(CONST4*CONST3)/SIN(CONST3)
117.      CONST6=-CJJ(J,J1)+(LJJK(J,J1,K)+KJJK(J,J1,K))*RJ/2.
118.      TERM=TERM+AJ1*CONST5*CEXP(CMPLX(0.,-CONST*CONST6))
119.      470  CONTINUE
120.      TKJ=RI0(J)-RIK(J,IK)
      C- ADD HASH TERM AND LEADING TERM
121.      CONST7=AJ*CEXP(CMPLX(0.,-CONST*TKJ))
122.      SUM2=SUM2+TERM*CONST7
123.      SUM=SUM+AJ*513.+CONST7
      C- NOW MULTIPLY BY EXP((-NU*TAU/2)**2)
124.      480  CONTINUE
125.      FKC(I)=(SUM+SUM2)*CONST1
126.      THAS(I)=SUM2*CONST1
127.      NU=NU+DELTANU
128.      490  CONTINUE
129.      WRITE(6,510) IK1
      C- COMPUTE FFT
130.      NTAPE=0
131.      CALL FFT(NSTAGE,1.0,FKC)
132.      CALL FFT(NSTAGE,1.0,THAS)
      C- SHIFT IN TIME
133.      CALL SH(NIT,FKC)
134.      CALL SH(NIT,THAS)
      C- PRINT OUT
135.      510  FORMAT(/// * ARRAY ELEMENT =*,I5/)
136.      WRITE(6,520)
137.      520  FORMAT(/12X,*T*,10X,*FK(T)*,10X,*HASH*//)
138.      521  FORMAT(/12X,*NU*,10X,*REAL(FK)*,10X,*IM(FK)*//)
139.      DELTAT=2.*TMAX/NIT
140.      T=TMAX
141.      DO 550 I=1,NIT
142.      YH(I)=CABS(THAS(I))
143.      YP(I)=CABS(FKC(I))
144.      WRITE(6,540) T,YP(I),YH(I)
145.      540  FORMAT(1X,F15.5,2E15.5)
146.      541  FORMAT(1X,F15.5,2E15.5)
147.      T=T+DELTAT
148.      550  CONTINUE
149.      CALL PLOT(YP,NIT,XMAX)
150.      CALL PLOT(YP,NIT,XMAX1)
151.      CALL PLOT(YH,NIT,-1.)
152.      999  CONTINUE
153.      STOP
154.      END

```


THIS PAGE IS BEST QUALITY PRACTICABLE
FROM COPY FURNISHED TO DDG

```

1.  SUBROUTINE FFT(NSTAGE,RSIGN,X)
    C  COPYRIGHT 1973 BY J. PRESTCOTT AND R. J. JENKINS
    C  DEPARTMENT OF ELECTRICAL ENGINEERING SCIENCE
    C  UNIVERSITY OF ESSEX      COLCHESTER      ESSEX
    C
    C  THIS SUBROUTINE MAY NOT BE USED FOR COMMERCIAL PURPOSES
    C  WITHOUT THE EXPRESS WRITTEN PERMISSION OF THE ABOVE.
    C
    C  THIS SUBROUTINE IMPLEMENTS A FAST FOURIER TRANSFORM
    C  ALGORITHM GIVEN BY M. L. UHRICH (IEEE TRANS. AUDIO AND
    C  ELECTROACOUSTICS, JUNE 1969, 170-172) ; AND W. T. COCHRAN
    C  ET AL (PROC. IEEE, OCT. 1967, 55:1664-1674).
    C
    C  THIS SUBROUTINE IS CALLED BY
    C
    C      CALL FFT(NSTAGE,RSIGN)
    C
    C  WHERE NSTAGE IS THE LOG (BASE 2) OF THE NUMBER OF POINTS IN
    C  THE TRANSFORM, SO THAT FOR 128 POINTS NSTAGE=7.
    C  THE SIGN GOVERNS THE DIRECTION OF THE TRANSFORM, AND IS
    C
    C      -1.0    FOR FORWARD TRANSFORMS
    C      +1.0    FOR INVERSE TRANSFORMS
    C  FIRST N LOCATIONS OF ARRAY X. THE NORMALIZED FORWARD
    C  TRANSFORM OR THE INVERSE TRANSFORM WILL APPEAR IN THE
    C  THE N COMPLEX POINTS OF THE INPUT SAMPLE SHOULD BE IN THE
    C
    C  CORRECT ORDER IN THE SAME N LOCATIONS.
    C
    C  THE SAMPLE ARRAY X IN COMFFT MUST HAVE AT LEAST 2*N ELEMENTS
    C  AND THE COEFFICIENT ARRAY T MUST HAVE AT LEAST N ELEMENTS.
    C
    C  THE SUBROUTINE STANDS ALONE AND CAN BE USED FOR ANY
    C  COMBINATION OF FORWARD AND INVERSE TRANSFORMS OF ANY SIZE,
    C  WITHOUT OUTSIDE ATTENTION.
    C
2.  COMPLEX X,W,TX1,TX2,T
3.  INTEGER SRC1,SRC2,DST1,DST2
4.  COMMON/COMFFT/T(1024),NTABLE
5.  DIMENSION X(2048)
6.  DATA NTABLE/0/
7.  TPI=9.0*ATAN(1.0)
    C
    C  COMPUTE COEFFICIENT TABLE AND SET NTABLE TO PREVENT
    C  RECALCULATION ON SUBSEQUENT CALLS TO THE SUBROUTINE.
    C
8.  IF(NTABLE.GT.0) GO TO 30
9.  PP=0.0
10. DO 20 I=1,512
11.  T(I)=CMPLX(COS(PP),SIN(PP))
12.  T(512+I)=CONJG(T(I))
13.  20  PP=PP-TPI/1024.0
14.  NTABLE=1024
15.  30  CONTINUE
    C
    C  SET UP THE LOOP CONTROL VARIABLES
    C

```

THIS PAGE IS BEST QUALITY PRACTICABLE
FROM COPY FURNISHED TO DDC

```

16.      INCR=NTABLE
17.      INDXIT=1
      C
      C      FOR INVERSE TRANSFORMS SELECT THE COMPLEX CONJUGATE TABLE
      C
18.      IF(PSIGN.GT.0.0) INDXIT=(NTABLE/2)+1
19.      N=2**NSTAGE
20.      N2=N/2
21.      JLIMIT=1
22.      KLIMIT=N
      C
      C      SET DST2 TO N (0) FOR NSTAGE ODD (EVEN) TO GOVERN THE
      C      CORRECT ALTERNATION OF COMPUTATION BETWEEN HALVES OF THE
      C      ARRAY
      C
23.      DST2=N.AND.(8192+2048+512+128+32+8)
      C
      C      IF AN INVERSE TRANSFORM, THE NORMALISATION LOOP WILL BE
      C      OMITTED, SO CHANGE THE ALTERNATION SEQUENCE.
      C
24.      IF(RSIGN.GT.0.0) DST2=DST2.XOR.N
25.      SRC2=0
      C
      C      OUTER LOOP
      C
26.      DO 3 I=1,NSTAGE
27.      KLIMIT=KLIMIT/2
28.      INCR=INCR/2
29.      INDX=INDXIT
      C
      C      ALTERNATE THE COMPUTATION BETWEEN SUBARRAYS AS REQUIRED.
      C
30.      DST1=DST2.AND.N
31.      SRC2=(SRC2.AND..NOT.DST1).AND.N
32.      DST2=DST1+N2
      C
      C      MIDDLE LOOP SELECTS THE COEFFICIENT
      C
33.      DO 2 J=1,JLIMIT
34.      SRC1=SRC2
35.      SRC2=SRC2+KLIMIT
36.      W=1(INDX)
      C      INNER LOOP
      C
37.      DO 1 K=1,KLIMIT
38.      SRC1=SRC1+1
39.      SRC2=SRC2+1
40.      DST1=DST1+1
41.      DST2=DST2+1
42.      TX1=X(SRC1)
43.      TX2=W*X(SRC2)
44.      X(DST1)=IX1+TX2
45.      1  X(DST2)=TX1-TX2
46.      2  INDX=INDX+INCR
47.      3  JLIMIT=JLIMIT+JLIMIT
      C
      C      IF FORWARD TRANSFORM THEN NORMALISE
      C
48.      IF(RSIGN.GT.0.0) RETURN
49.      PP=1.0/FLOAT(N)
50.      DO 4 I=1,N
51.      4  X(I)=X(N+1)*PP
52.      RETURN
53.      END

```

THIS PAGE IS BEST QUALITY PRACTICABLE
FROM COPY FURNISHED TO DDG

```

1.      SUBROUTINE PLOT(X,NN,XMAX)
C- PLOTS N POINTS IN X ON PRINTER. XMAX IS X VALUE WHICH
C- IS TO BE MAXIMUM ON PLOT. IF XMAX .LE. 0, PROGRAM WILL
C   USE LARGEST VALUE IN X AS XMAX
2.      DIMENSION X(1),CHAR(100)
3.      INTEGER BLANK,PL,CHAR
4.      DATA NCOL/100/
5.      N=NN
6.      PL=1H*
7.      BLANK=1H
8.      WRITE(6,1)
C- IF XMAX .LE. 0 MAXIMIZE X ARRAY TO GET XMAX
9.      IF(XMAX.GT.0) GO TO 10
10.     DO 2 I=1,N
11.     IF(X(I).GT.XMAX) XMAX=X(I)
12.     2   CONTINUE
C- NOW FILL CHAR BUFFER
13.     10  DO 50 I=1,N
14.     IX=(X(I)/XMAX)*NCOL
15.     IF(IX.GT.100) IX=100
16.     IF(IX.LT.0) IX=0
17.     DO 20 II=1,NCOL
18.     20  CHAR(II)=BLANK
19.     IF(IX.EQ.0) GO TO 40
20.     DO 30 II=1,IX
21.     CHAR(II)=PL
22.     30  CONTINUE
C- PRINT LINE
23.     40  IF(IX.EQ.0) CHAR(1)=1HI
24.     1   FORMAT(//1X,*-----*)
25.     WRITE(6,100) CHAR
26.     50  CONTINUE
27.     100 FORMAT(1X,100A1)
28.     WRITE(6,1)
29.     RETURN
30.     END

```


Appendix II

Listing of the Program
to Simulate Reverberation Environment

TABLE 1

THIS PAGE IS BEST QUALITY PRACTICABLE
FROM COPY FURNISHED TO DDC

```

1.  PROGRAM I46(TAPE17,TAPE18,TAPE19,OUTPUT,TAPE6=OUTPUT)
2.  COMMON /K, 2n),RK(K,1000),Q(1000)
3.  DIMENSION X(1000),R(2000),F( 2n),T( 2n),SEED(3)
4.  DIMENSION Y( 2n)
5.  DIMENSION EX(100),AL(100)
6.  COMPLEX Y,Z,TEMP,TK,EX
7.  INTEGER S,T
8.  DATA TW,R0,K,S,N/open
9.  PI=4.0*ATAN(1.0)
10. P=2*PI
11. LL=4*K
12. DF=1.0/11704.0
13. SEED(1)=0.0
14. SEED(2)=1.0
15. CALL RAN3F(-2000,R,SEED)
16. CALL RAN3F(2000,R,SEED)
17. DO 17 I=1,N
18.   R(I)=R0+1000*P(I)-500
19.   X(I)=2000*R(I+1)-1000
20.   AB=R(I)**2+A(I)**2
21.   R(I)=SORT(AB)
22.   Q(I)=X(I)/R(I)
23.   DO 7 J=1,K
24.     7 RK(J,I)=R(I)-(J-16)*Q(I)
25. 17 CONTINUE
26. DO 1 I=1,100
27.   1 EX(I)=CEXP(COMPLX(0.0,P*(.01*I-.005)))
28. DO 3 I=1,LL
29.   F(I)=1+(I-LL/2)*DF
30.   3 T(I)=EXP(-(PI*(1-F(I))*TW)**2)
31. DO 11 KK=1,K
32. DO 10 I=1,LL
33. DO 2 J=1,100
34.   2 AL(J)=0.0
35. DO 5 J=1,N
36.   D=F(I)*(RK(RK,J)+R(J))
37.   M=(D-INT(D))*100+1
38.   5 AL(M)=AL(M)+1
39. Y(I)=(0.0,0.0)
40. DO 6 J=1,100
41.   6 Y(I)=Y(I)+AL(J)*EX(J)
42. Y(I)=Y(I)*T(I)
43. Z(RK,I)=Y(I)
44. 10 CONTINUE
45. 11 CONTINUE
46. WRITE(17)((Z(J,I),J=1,32),I=1,128)
47. STOP
48. END

```

TABLE 2

THIS PAGE IS BEST QUALITY PRACTICABLE
FROM COPY FURNISHED TO DDG

1.		PROGRAM IM6(TAPE17,TAPE18,TAPE19,OUTPUT,TAPE6=OUTPUT)
2.		COMMON Z(K,2 ⁿ),T(2 ⁿ),F(2 ⁿ)
3.		DIMENSION Y(2 ⁿ)
4.		COMPLEX Z,Y
5.		INTEGER S,TW
6.		DATA TW,R0,K,S,N/160,1000.0,32,15,1000/
7.		READ(17)((Z(J,I),J=1,32),I=1,128)
8.		PI=4.0*ATAN(1.0)
9.		P=2*PI
10.		LL=4*K
11.		DF=1.0/11704.0
12.		DO 4 I=1,LL
13.		F(I)=1+(I-LL/2)*DF
14.	3	T(I)=EXP(-(PI*(1-F(I))*TW)**2)
15.		D=2*R0*F(I)
16.		D=P*(D-INT(D))
17.	4	Y(I)=T(I)*S*CEXP(CMPLX(0.0,D))
18.		DO 100 I=1,LL
19.		DO 80 J=1,K
20.	80	Z(J,I)=Z(J,I)+Y(I)
21.	100	CONTINUE
22.		WRITE(18)((Z(J,I),J=1,K),I=1,2 ⁿ)
23.		STOP
24.		END

TABLE 3

THIS PAGE IS BEST QUALITY PRACTICABLE
FROM COPY FURNISHED TO DDC

```

1. PROGRAM IM3(TAPE17,TAPE21,TAPE20,OUTPUT,TAPE6=OUTPUT)
2. COMMON 7(K,2N),Q(1000),X(1000),R(2000)
3. DIMENSION F(2N),Y(2N),SEED(3)
4. DIMENSION EX(100),AL(100)
5. COMPLEX Y,Z,TEMP,TK,EX
6. INTEGER S,TW
7. DATA TW,R0,K,S,N/
8. READ(17)((Z(J,I),J=1,32),I=1,128)
9. PI=4.0*ATAN(1.0)
10. P=2*PI
11. LL=4*K
12. DF=1.0/11704.0
13. SEED(1)=0.0
14. SEED(2)=1.0
15. CALL RAN3F(-2000,R,SEED)
16. CALL RAN3F(2000,R,SEED)
17. DO 17 I=1,N
18. R(I)=R0+1000*R(I)-500
19. X(I)=2000*R(N+I)-1000
20. AB=R(I)**2+X(I)**2
21. R(I)=SQRT(AB)
22. Q(I)=X(I)/R(I)
23. 17 CONTINUE
24. CALL NORMAL(-1000,X,SEED)
25. CALL NORMAL(1000,X,SEED)
26. DO 3 I=1,LL
27. 3 F(I)=1+(I-LL/2)*DF
28. DO 1 I=1,100
29. 1 EX(I)=CFXP(CMPLX(0.0,-P*(.01*I-.005)))
30. DO 90 II=1,LL
31. I=LL+1-II
32. DO 30 KK=-30,32
33. DO 2 J=1,100
34. 2 AL(J)=0.0
35. DO 5 J=1,N
36. D=F(I)*(2*R(J)-KK*Q(J)+X(J))
37. M=(D-INT(D))*100+1
38. 5 AL(M)=AL(M)+1
39. Y(KK+31)=(0.0,0.0)
40. DO 6 J=1,100
41. 6 Y(KK+31)=Y(KK+31)+AL(J)*EX(J)
42. 30 CONTINUE
43. DO 55 KK=1,K
44. TK=(0.0,0.0)
45. DO 40 K1=1,K
46. 40 TK=TK+7(K1,I)*Y(KK+K1-1)
47. 55 WRITE(21)TK
48. 90 CONTINUE
49. STOP
50. END

```

THIS PAGE IS BEST QUALITY PRACTICABLE
FROM COPY FURNISHED TO DDC

TABLE 4

```

1. PROGRAM IM10(TAPE22,TAPE23,OUTPUT,TAPE6=OUTPUT)
2. COMMON / (K, 2n), Q(1000), X(1000), R(2000)
3. DIMENSION F( 2n), Y( 2n), SEED(3)
4. DIMENSION EX(100), AL(100)
5. COMPLEX Y,Z,TEMP,TK,EX
6. INTEGER S,TW
7. DATA TW,R0,K,S,N/ .....
8. READ(22)((Z(J,I),J=1,32),I=1,128)
9. PI=4.0*ATAN(1.0)
10. P=2*PI
11. LL=4*K
12. DF=2.0/11704.0
13. SEED(1)=0.0
14. SEED(2)=1.0
15. CALL RAN3F(-2000,R,SEED)
16. CALL RAN3F(2000,R,SEED)
17. DO 17 I=1,N
18. R(I)=R0+1000*R(I)-500
19. X(I)=2000*R(N+I)-1000
20. AB=R(I)**2+X(I)**2
21. R(I)=SQRT(AB)
22. Q(I)=X(I)/R(I)
23. 17 CONTINUE
24. CALL NORMAL(-1000,X,SED)
25. CALL NORMAL(1000,X,SED)
26. DO 3 I=1,LL
27. 3 F(I)=1+(I-LL/2)*DF
28. DO 1 I=1,100
29. 1 EX(I)=C*EXP(CMPLX(0.0,-P*(.01*I-.005)))
30. DO 90 II=1,LL
31. I=LL+1-II
32. TEMP=(0.0,0.0)
33. DO 20 KK=1,K
34. 20 TEMP=TEMP+Z(KK,I)
35. D=2*R0*F(I)
36. D=-P*(D-INT(D))
37. TEMP=TEMP+S*CEXP(CMPLX(0.0,D))
38. DO 30 KK=-30,32
39. DO 2 J=1,100
40. 2 AL(J)=0.0
41. DO 5 J=1,N
42. D=F(I)*(2*R(J)-KK*Q(J)+X(J))
43. M=(D-INT(D))*100+1
44. 5 AL(M)=AL(M)+1
45. Y(KK+31)=(0.0,0.0)
46. DO 6 J=1,100
47. 6 Y(KK+31)=Y(KK+31)+AL(J)*EX(J)
48. 30 CONTINUE
49. DO 55 KK=1,K
50. TK=(0.0,0.0)
51. DO 40 K1=1,K
52. 40 TK=TK+7*(K1,I)*Y(KK+K1-1)
53. TK=TK+TEMP
54. 55 WRITE(23)TK
55. 90 CONTINUE
56. STOP
57. END

```

TABLE 5

1.		PROGRAM IM6(TAPE17,TAPE18,TAPE19,OUTPUT,TAPE6=OUTPUT)
2.		COMMON Z(32,128),A(4096)
3.		DIMENSION Y(128),T(128)
4.		DIMENSION IW(100),W(100)
5.		LOGICAL LF(100)
6.		EQUIVALENCE (IW(1),W(1),LF(1))
7.		COMPLEX Y,Z,IT,TEMP
8.		LL=128
9.		DT1=11704.0/256.0
10.		READ(18)((Z(J,I),J=1,32),I=1,128)
11.		DO 15 J=0,31
12.		DO 5 I=1,128
13.	5	Y(I)=Z(J+1,I)
14.		DO 33 I=1,LL/2
15.		TEMP=Y(I)
16.		Y(I)=Y(LL/2+I)
17.	33	Y(LL/2+1)=TEMP
18.		DO 25 KK=1,LL
19.	25	Y(KK)=CONJG(Y(KK))
20.		CALL FFTP(Y,LL,IW,W,LF)
21.		DO 37 I=1,LL/2
22.		TEMP=Y(I)
23.		Y(I)=Y(LL/2+I)
24.	37	Y(LL/2+1)=TEMP
25.		DO 10 I=1,128
26.	10	A(128+J+1)=CABS(Y(I))
27.	15	CONTINUE
28.		CALL PLOTS(1,-1,13HPROF. MUELLER,70.0,3HIM2)
29.		CALL SCALE(A,4096,1,1.0,AMIN,DA)
30.		DO 45 J=0,31
31.		T(1)=-DT1*(LL/2-1)-DT1/2
32.		DO 18 I=2,LL
33.	18	T(I)=T(I-1)+DT1
34.		CALL SCALE(T,LL,1,7.5,TMIN,DT2)
35.		CALL PLOT(T(1),A(128+J+1),3)
36.		DO 20 I=2,128
37.	20	CALL PLOT(T(I),A(128+J+1),2)
38.		CALL PLOT(0.0,1.0,-3)
39.	45	CONTINUE
40.		CALL PLOTS(-1)
41.		STOP
42.		END